# A comprehensive survey of artificial intelligence-based techniques for performance enhancement of solid oxide fuel cells: Test cases with debates

**Hossam Ashraf[1] · Abdelmonem Draz[2]**

## Abstract

Since installing solid oxide fuel cells (SOFCs)-based systems suffers from high expenses, accurate and reliable modeling is heavily demanded to detect any design issue prior to the system establishment. However, such mathematical models comprise certain unknowns that should be properly estimated to effectively describe the actual operation of SOFCs. Accordingly, due to their recent promising achievements, a tremendous number of metaheuristic optimizers (MHOs) have been utilized to handle this task. Hence, this effort targets providing a novel thorough review of the most recent MHOs applied to define the ungiven parameters of SOFCs stacks. Specifically, among over 300 attempts, only 175 articles are reported, where thirty up-to-date MHOs from the last five years are comprehensively illustrated. Particularly, the discussed MHOs are classified according to their behavior into; evolutionary-based, physics-based, swarm-based, and nature-based algorithms. Each is touched with a brief of their inspiration, features, merits, and demerits, along with their results in SOFC parameters determination. Furthermore, an overall platform is constructed where the reader can easily investigate each algorithm individually in terms of its governing factors, besides, the simulation circumstances related to the studied SOFC test cases. Over and above, numerical simulations are also introduced for commercial SOFCs' stacks to evaluate the proposed MHOs-based methodology. Moreover, the mathematical formulation of various assessment criteria is systematically presented. After all, some perspectives and observations are provided in the conclusion to pave the way for further analyses and innovations.

---

✉ Hossam Ashraf
    Hossam.Ashraf@bue.edu.eg

1   Electrical Engineering Department, Faculty of Engineering and FabLab in the Centre for Emerging Learning Technologies (CELT), The British University in Egypt (BUE), Cairo, Egypt

2   Electrical Power and Machines Department, Zagazig University, Zagazig 44519, Egypt

# 1 Introduction

Nowadays, the prompt growth of the world economy reveals the heavy need for sustainable and secure energy sources (Mehran et al. 2023). In other words, the dependence on fossil fuels has become a major obstacle to continuous economic development due to their shortage, high price, and ecological ruinous impacts (Jolaoso et al. 2023; Lamagna et al. 2023). Thus, exploiting renewable energy sources (RESs), such as wind and solar, is compulsory for a smooth transition toward a technological global renaissance (Kasaeian et al. 2023; Yatoo et al. 2023). Besides, the expansion of installing RESs significantly reduces greenhouse emissions, which supports international endeavors to mitigate global warming issues (Lee et al. 2023a, b). Among the various RESs, fuel cells (FCs) have a very incremental rate of utilization in power systems as a result of their environmentally friendly nature and high transformation efficiency (Jawad et al. 2022; Lokhande et al. 2023). However, the researchers along with the industry stakeholders are persistently seeking to discover alternative raw substances and innovate new fabrication techniques for diminishing the FC's cost (Ghavidel and Mousavi-G 2022; Rupiper et al. 2022).

Recently, FC systems have been involved in numerous commercial applications, beginning with the power generation units, passing through the transportation facilities, and ending up with the portable applications (Lee et al. 2023a, b; Yang et al. 2021a, b, c). According to the electrolyte material, FCs have diverse types, like proton exchange membrane FC (PEMFC) (Ashraf et al. 2022b), solid oxide FC (SOFC) (Fathy et al. 2020), alkaline FC (AFC) (Hamada et al. 2023), molten carbonate FC (MCFC) (Cigolotti et al. 2021), and many more (Inci and Türksoy 2019; Sazali et al. 2020). Particularly, the main features of some well-known FC's types are captured in Table 1 (Ashraf et al. 2022a). More specifically, SOFC is distinguished by a higher conversion efficiency and more fuel resiliency than the other candidates. Consequently, it plays a vital role in replacing internal combustion engine-propelled vehicles with electric vehicles where SOFC is employed as the principal propulsion source (Bessekon et al. 2019; Ren 2022). On top of this, due to its high operating temperature that yields a large amount of unused heat, it's considerably engaged in the combined cycle of power plants (Oryshchyn et al. 2018).

In fact, it's obvious that SOFCs are generally utilized in bulky projects (Perna et al. 2018). So, such systems shall be brought to study, analysis, and validation to catch up with any design flaws prior to starting the costly installation (Ashraf et al. 2022a, b, c; Wu et al. 2019). Hence, modeling SOFCs is imperative to accurately describe their performance, in terms of the electrical behavior (V-I and P-I curves), during different operating and faulty conditions (Ghanem et al. 2022; Lee et al. 2022). Additionally, SOFCs modeling enables precise simulation of the internal physical phenomena, perfect control, and efficient prediction of their response to unanticipated events during operation (Safari et al. 2018). Nevertheless, proper modeling is a challenging task due to the ingrained nonlinearity and nonconvexity that portray their dynamic performance (de Melo et al. 2018). Thus, several models have been proposed lately, which can be classified based on many aspects, like the derivation technique (empirical, semi-empirical, or analytical), and the discussed phenomena (electrochemistry or mass and heat transport) (Prokop et al. 2018; Rossi et al. 2019; Zhu et al. 2021). Also, SOFC models can be categorized based on the performance scale (cell, stack, or system) and the operation state (steady or dynamic). Notwithstanding, most of these categories share a significant property which is their containment of a group of unknown parameters that should be optimally assigned (Karanfil 2020).

**Table 1** Practical features of some FC's types

| FC type | Electrolyte substance | Fuel | Oxidant | Operating temperature (K) | Efficiency (%) | Output power (MW) | Capital cost ($/W) | Advantages | Drawbacks |
|---|---|---|---|---|---|---|---|---|---|
| PEMFC (Ashraf et al. 2022b; Cigolotti et al. 2021) | Solid Nafion | Hydrogen | Oxygen/ Air | 333–353 | 40–60 | ≥0.1 | 0.1 | • High power density and electrical efficiency • Compact and modular shape • Fast startup time | • High sensitivity to carbon monoxide • Complicated heat and water management • Expensive catalyst |
| SOFC (Fathy et al. 2020; Inci & Türksoy 2019) | Solid yttria/ stabilized zirconia (ZrO-Y$_2$O$_3$) | Methane/ natural gas/ coal gas | Oxygen/ Air | 1073–1273 | 55–70 | 0.001–2 | 1 | • High power and current density • High thermal level • Suitable for internal reforming | • Slow startup response • High fabricating cost • High thermal stress |
| AFC (Hamada et al. 2023; Sazali et al. 2020) | Sodium hydroxide (NAOH)/ potassium hydroxide (KOH) | Hydrogen | Refined oxygen | 353–503 | 60–70 | 0.001–0.1 | 0.05–0.1 | • Wide scale of operating temperatures and pressures • Resilient and low-cost catalyst • High electrical efficiency | • Modest power density • Extremely sensitive to pollutants • High corrosion rate of the electrolyte |

**Table 1** (continued)

| FC type | Electrolyte substance | Fuel | Oxidant | Operating temperature (K) | Efficiency (%) | Output power (MW) | Capital cost ($/W) | Advantages | Drawbacks |
|---|---|---|---|---|---|---|---|---|---|
| MCFC (Ashraf et al. 2022a; Cigolotti et al. 2021) | Alkalicarbonate ($K_2CO_3$) | Methane/ natural gas/ coal gas | Oxygen/ Air | 873–973 | 55–65 | 0.5–10 | 1 | • High electrical efficiency<br>• High thermal level<br>• Suitable for internal reforming | • Slow startup response<br>• High corrosion rate of the electrolyte<br>• Vaporization losses |

Consequently, tremendous attempts have been executed to accurately specify such parameters. For example, electrochemical impedance spectroscopy (Cao et al. 2010) and fractional derivative techniques have been employed for identifying the transient model (Caliandro et al. 2019). On the other hand, the receding-horizon experiment has been applied for the online parameter estimation of real time model (Yang et al. 2020a, b). Nonetheless, such traditional optimizers lack fast and stable computation over all scenarios due to their complicated structure and reliance on the initial conditions. In addition, the undefined parameters in SOFC models are strongly coupled with the operating circumstances resulting in a heavier burden optimization task. Therefore, finding novel, effective, and robust optimization methods to deal with such a tricky task becomes inevitable (Ohenoja and Leiviskä 2020; Priya et al. 2018; Yang et al. 2020).

Since the overwhelming evolution of the computer-based applications, metaheuristic optimizers (MHOs) have achieved a good reputation in tackling diverse extreme nonlinear optimization problems (Alsaidan et al. 2022; Mitra et al. 2023; Zhou et al. 2024). They prove their competency and reliability to offer optimal solutions for highly sophisticated tasks with few requirements when compared to conventional optimizers (Kahia et al. 2023; Korkmaz et al. 2023; Sarmah et al. 2017). Indeed, the parameter estimation of SOFC can be principally regarded as an optimization task, where a vast number of MHOs have been adopted to optimally allocate the ungiven parameters with low computational burden and high efficacy (Gong et al. 2014; Jia and Taheri 2021; Xiong et al. 2021).

Again, such optimization techniques are utilized to promote the modelling accuracy of SOFCs. Principally, MHOs are engaged to enhance the mathematical models in a way that they can precisely describe the actual behavior of SOFCs when subjected to diverse operating conditions. Consequently, this not only will lead to better design and implementation of SOFC-based systems but also will allow optimal prediction of SOFC performance due to any sudden circumstances.

Generally speaking, MHOs are not only used for parameter identification of SOFCs, but also are dedicated for further analysis and investigation of power system problems (Draz et al. 2021). Many frameworks related to power systems design, operation, control, protection, and more have been formulated and solved using MHOs. To name just a few, protection coordination of overcurrent relays (Draz et al. 2023a, b), optimal power flow (El-Fergany and Hasanien 2015), energy management strategies (Emad et al. 2021), and optimal allocation of distributed generators (El-Fergany 2015) represent some models in electric power systems. Moreover, the performance of MHOs is assessed for solving the problems of parameter estimation of PEMFCs (Ashraf et al. 2022a), photovoltaic cells (El-Fergany 2021), and batteries (Hasanien et al. 2023). Even though, these models may be reformulated for different objectives such as integration of fast charging stations (Draz et al. 2023a, b), frequency control (El-Hameed and El-Fergany 2016), and renewables' integration in modern power systems (Elkholy et al. 2018). In this context, Fig. 1 summarizes most of MHO's applications for solving the earlier mentioned problems in electric power systems.

Regarding SOFC's optimization, the authors in (Yang et al. 2020a, b) present a literature review of the application of MHOs in the SOFC parameters estimation. However, it only discusses seventeen MHOs without categorizing them according to their inspiration. Moreover, the authors didn't go deep into stating the simulation settings of such algorithms, like the iteration number, population size, and other tunable factors. Thence, this article introduces a comprehensive survey to summarize the outcomes of several MHOs engaged in the parameter identification of SOFC models. In this regard, 175 up-to-date articles are documented to construct this survey, where their annual distribution is revealed in Fig. 2.

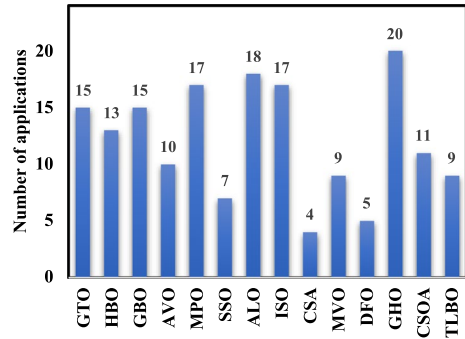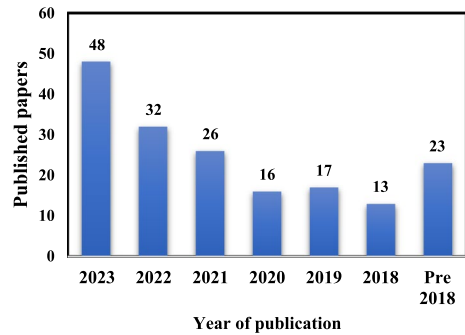**Fig. 1** Numerical statistic of MHOs' applications on power systems



**Fig. 2** Numerical statistic of published papers per year



Specifically, the major contributions can be listed as follows:

(i)　A detailed mathematical representation of various well-known SOFC models, along with a brief comparison, is offered,

(ii)　An intensive discussion of thirty up-to-date MHOs utilized in SOFC parameter estimation is introduced,

(iii)　Besides, a comprehensive summary, comprises their simulation settings and outcomes, is also elaborated,

(iv)　Additionally, a fair and precise statistical comparison of such optimizers is conducted to accurately assess their computational performance, and

(v)　Finally, two well-reputed SOFC test cases are evaluated to validate the effectiveness of the proposed MHOs-based methodology.

The remainder of this paper is structured as follows: various mathematical modelling techniques of SOFC are presented in Sect 2. Several assessment criteria that have been adopted in SOFC parameter identification are discussed in Sect 3. Section 4 reveals a thorough review of thirty recent MHOs in terms of their inspiration, description, and results in SOFC parameter recognition. A validating discussion to assess the

accuracy of such algorithms is introduced in Sect 5. Future insights and research directions are announced in Sect 6. Lastly, Sect. 7 provides the conclusion.

## 2 Mathematical formulation of solid oxide fuel cell

As mentioned earlier, precise and efficient modeling is substantial to actually emulate the SOFC performance over a wide range of operating instants. Therefore, a plentiful number of mathematical models have been proposed to accurately imitate various SOFC operation aspects, especially the polarization characteristics (V-I and P-I curves) (Gong et al. 2014; Jia and Taheri 2021; Xiong et al. 2021; Yang et al. 2020a, b). In this context, this section illustrates the operation theory of SOFCs along with their construction. In addition, it brings up to the reader the most well-known models that effectively describe the electrical characteristics of SOFCs either in steady-state or dynamic operation.

### 2.1 Operation Theory

Basically, a practical SOFC consists of three regions, the anode, the cathode, and the electrolyte bounded between them, as shown in Fig. 3 (Jia and Taheri 2021). In fact, the electrochemical reactions that take place in anode–cathode structure are formulated in (1) and (2), respectively.
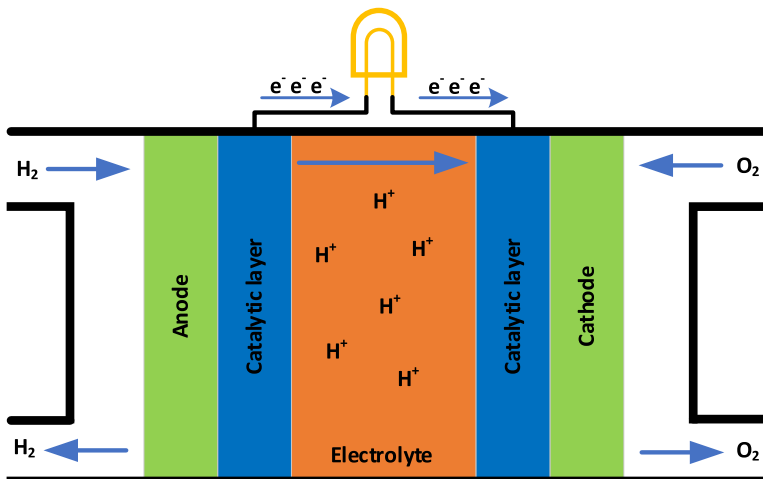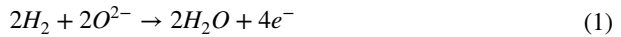
$$2H_2 + 2O^{2-} \rightarrow 2H_2O + 4e^- \tag{1}$$

$$O_2 + 4e^- \rightarrow 2O^{2-} \tag{2}$$
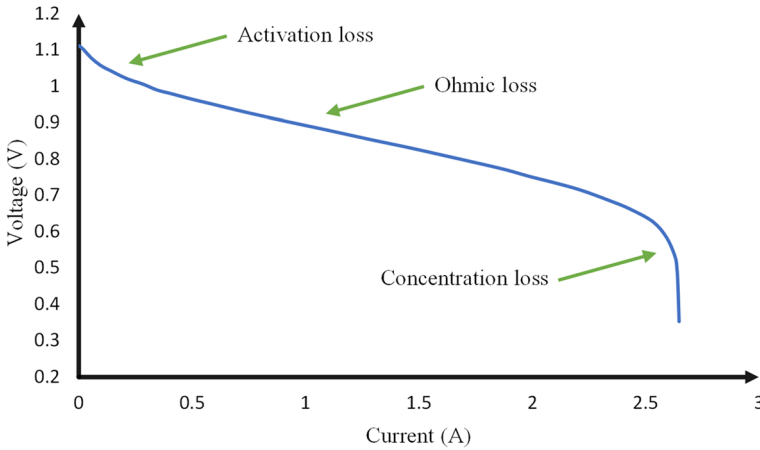


**Fig. 3** Basic construction of SOFC

**Fig. 4** Typical V-I curve of SOFC

## 2.2 Electrochemical Model

Mainly, the output voltage of SOFC is experienced by three polarization losses, activation overpotential $V_{ac}$ in $(V)$, ohmic voltage drop $V_{oh}$ in $(V)$, and concentration loss $V_{cn}$ in $(V)$, as indicated in Fig. 4 (Xiong et al. 2021). In fact, the activation overpotential refers to the initial slowness of the chemical reactions. Whereas the voltage decay due to the electrolyte and external connections resistance is defined by the ohmic voltage drop. Lastly, the mass transport phenomenon yields concentration losses. So, the best harmony between the experimental polarization curve and the model-generated one heavily relies on the optimal allocation of the model's unknown parameters (Zhu et al. 2015).

Generally, a group of series connected SOFCs is called a stack. In this context, all the subsequent models assume the same mathematical formulation of the stack output voltage $V_{sk}$ in $(V)$, as given by (3) (Noren and Hoffman 2005).

$$V_{sk} = N_{cl} \cdot \left( V_{nr} - V_{ac} - V_{oh} - V_{cn} \right) \tag{3}$$

where, $N_{cl}$ is the number of connected SOFCs. $V_{nr}$ symbolizes the Nernst open-circuit voltage in $(V)$ and is given by (4).

$$V_{nr} = V_o + \frac{RT_{op}}{2F} ln \left[ \frac{(P_H)^2 P_O}{(P_W)^2} \right] \tag{4}$$

where, $V_o$ is the reversable reference voltage in $(V)$, $R = 8.314 J/(mol.K)$ is the universal gas constant, $F = 96485 C/mol$ is the Faraday constant, and $T_{op}$ denotes the stack operating temperature in $(K)$. $P_H$, $P_O$, and $P_W$ refer to the hydrogen, oxygen, and water partial pressures in $(atm)$.

Additionally, Using Bulter-Volmer equation, the activation voltage drop can be described by (5).

$$V_{ac} = A. \left\{ \sinh^{-1} \left[ \frac{J_{ld}}{2J_{ex,a}} \right] + \sinh^{-1} \left[ \frac{J_{ld}}{2J_{ex,c}} \right] \right\} \tag{5}$$

where, the load current density is represented by $J_{ld}$ in $(A.cm^{-2})$. The exchange current densities of the anode and cathode are symbolized by $J_{ex,a}$ and $J_{ex,c}$ in $(A.cm^{-2})$, respectively. $A$ is Tafel line slope in $(V)$.

Moreover, the ohmic loss $V_{oh}$ can be expressed by (6).

$$V_{oh} = J_{ld} \times \mathfrak{R}_n \tag{6}$$

where, $\mathfrak{R}_n$ indicates the ionic resistance in $(k\Omega.cm^2)$.

Finally, the concentration overpotential $V_{cn}$ can be computed by (7).

$$V_{cn} = -Bln \left[ 1 - \frac{J_{ld}}{J_m} \right] \tag{7}$$

where, $B$ is a constant in $(V)$ and $J_m$ represents the maximum current density in $(A.cm^{-2})$.

Now, it's clear that there are seven unknowns should be optimally tuned, which are $V_{nr}$, $A$, $J_m$, $J_{ex,a}$, $J_{ex,c}$, $\mathfrak{R}_n$, and $B$.

## 2.3 Steady-State Model (1)

With a slight difference to the electrochemical model, this model defines the open circuit voltage $V_{nr}$ as in (8) (Gebregergis et al. 2008).

$$V_{nr} = V_o + \frac{RT_{op}}{4F} ln \left[ \frac{(P_H)^2 P_O}{(P_W)^2} \right] \tag{8}$$

However, $V_o$ refers here to the voltage dependence on temperature and is formulated by (9).

$$V_o = V_o^o - C_e \left( T_{op} - 298 \right) \tag{9}$$

where, $V_o^o$ denotes the voltage standard under nominal conditions $(T_{op} = 298K, P = 1atm)$ and $C_e$ is an empirical coefficient.

Herein, the activation voltage drop $V_{ac}$ can be simplified and written as in (10) (Chan et al. 2002).

$$V_{ac} = \frac{RT_{op}}{\ddagger F} \sinh^{-1} \left[ \frac{J_{ld}}{2J_{ex}} \right] \tag{10}$$

where, $\ddagger$ represents the number of travelling electrons per mole of suppliants ($\ddagger = 2$). The overall exchange current density is symbolized by $J_{ex}$ in $(A.cm^{-2})$ and given by (11)

$$J_{ex} = C_1.T_{op}.e^{(-C_2/T_{op})} \tag{11}$$

where, $C_1$ and $C_2$ are empirical coefficients.

Actually, the ohmic losses $V_{oh}$ is much detailed in this model, as indicated in (12).

$$V_{oh} = J_{ld}.C_3.e^{\left[C_4\left(\frac{1}{T_o} - \frac{1}{T_{op}}\right)\right]} \tag{12}$$

where, $C_3$, $C_4$, $T_o$ are material constants. Specifically, $C_3$ and $C_4$ calculate the inherent resistance of SOFC.

Lastly, the activation overpotential $V_{ac}$ can be derived from (13).

$$V_{cn} = \frac{RT_{op}}{\ddagger F} ln\left[1 - \frac{J_{ld}}{2J_m}\right] \tag{13}$$

where, the maximum current density $J_m$ is computed here by (14).

$$J_m = \frac{C_5}{T_{op}} ln\left[1 - Cn_s\right] \tag{14}$$

where, $C_5$ is a constant and $Cn_s$ represents the concentration of the suppliant.

Accordingly, there are six ungiven parameters, which are $C_e$, $C_1$, $C_2$, $C_3$, $C_4$, and $C_5$, have to be precisely determined in this model.

## 2.4  Steady-State Model (2)

Principally, this approach defines the no-load output voltage of SOFC $V_{nr}$ as in (15) (Bavarian et al. 2010).

$$V_{nr} = \frac{1}{\ddagger F}\left[-\Delta G°(T_{op}) + RT_{op} ln\left(\frac{P_H \sqrt{P_O}}{P_W}\right)\right] \tag{15}$$

where, $\Delta G°(T_{op})$ refers to the change in Gibbs free energy in (*Joule*).

Moreover, the activation voltage drop is described by Tafel equation and given by (16) (Yang et al. 2020a, b).

$$V_{ac} = A.\sinh^{-1}\left[\frac{J_{ld}}{2J_{ex}}\right] \tag{16}$$

It's worth noting that above formula is only applicable for $J_{ld} > J_{ex}$.

Fortunately, the ohmic and concentration losses in this model are the same as those defined in the electrochemical model and determined by (6) and (7), respectively.

Now, it's noticeable that only $V_{nr}$, $A$, $\Re_n$, $B$, $J_{ex}$, and $J_m$ are the targeted parameters to be optimized.

## 2.5  Dynamic Model

Basically, this mathematical approach provides a more realistic simulation of SOFC performance than the others. In fact, it takes into account the time constants of the fuel processors due to the alternation rate of the fuel pressures (Chakraborty 2009). Furthermore, it emulates the reliance of hydrogen, oxygen, and vapor pressures on the molar flowrate. Considering the same output voltage expressed in (15), the hydrogen pressure rate of change $\frac{dP_H}{dt}$ is formulated by (17) (Xu et al. 2016).

$$\frac{dP_H}{dt} = \frac{RT_{op}}{V_{an}}\left(q_H^{in} - C_H P_H - 2C_r J_{ld}\right) \tag{17}$$

where, $V_{an}$ is the anode volume in $(m^3)$, $q_H^{in}$ represents the input hydrogen flowrate in $(kmol/sec)$, $C_H P_H$ refers to the output hydrogen molar flowrate in $(kmol/sec)$, and the molar flowrate of the anode-reacted hydrogen is symbolized by $2C_r J_{ld}$ in $(kmol/sec)$. More specifically, $C_H$ denotes the constant of the hydrogen valve gain in $(kmol/atm.sec)$ and $C_r = \frac{N_{cl}}{F}$ in $(kmol/A.sec)$.

When taking Laplace transformation, the aforementioned formula can be determined by (18).

$$P_H(s) = \frac{\frac{1}{C_H}}{1 + \tau_H s}\left(q_H^{in} - 2C_r J_{ld}\right) \tag{18}$$

Adding to that, the Laplace domain for the oxygen and water vapor partial pressures is formulated by (19), (20), respectively. $\tau_H$ is the time constant of the hydrogen flow in $(sec)$.

$$P_O(s) = \frac{\frac{1}{C_o}}{1 + \tau_O s}\left(q_O^{in} - C_r J_{ld}\right) \tag{19}$$

$$P_W(s) = \frac{\frac{1}{C_W}}{1 + \tau_W s}\left(2C_r J_{ld}\right) \tag{20}$$

where, $C_O$ and $C_W$ are the constants of the oxygen and water vapor valve gains in $(kmol/atm.sec)$. $\tau_O$ and $\tau_W$ represent the time constants of the oxygen and water vapor flows in $(sec)$.

Lastly, the time delay of input hydrogen flowrate is structured as a 1st order in (21).

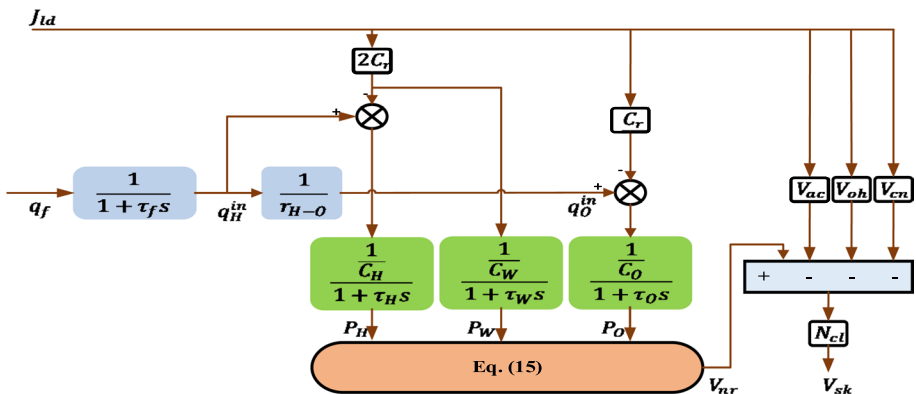$$q_H^{in}(s) = \frac{1}{1 + \tau_f s}\left(q_f\right) \tag{21}$$



**Fig. 5** Schematic diagram of SOFC transient model

where, $q_f$ refers to the fuel flowrate in ($kmol/s$) and $\tau_f$ is the time constant of the fuel processor in (*sec*).

For ease of illustration, the reader can refer to Fig. 5, where the schematic block diagram of the dynamic model is constructed. It's worth mentioning that the model demonstrates the transient responses due to load variations, while the variations of thermodynamics are neglected. Nevertheless, it contains the same sex unspecified parameters as steady-state model (2), which are $V_{nr}$, $A$, $\mathfrak{R}_n$, $B$, $J_{ex}$, and $J_m$.

To sum up, Fig. 6. offers a brief comparison of the basic features of the aforementioned SOFC models (Yang et al. 2020a, b).

## 3 Assessment Formulas

Since the unknown parameters are now located, it's time to formulate the evaluation criteria the optimizer will seek to minimize. Indeed, an assessment formula (AF) is a crucial factor in determining how efficiently the algorithm reaches the unknown's optimal values (Jia and Taheri 2021; Xiong et al. 2021). In this regard, Table 2 introduces a well-organized brief about the various objective functions captured in the literature in terms of their mathematical expressions, whether they use quadratic or absolute values, and variables' type. It can be concluded from Table 2 that some researchers employ absolute values to avoid the negative sign, while others apply the quadratic ones to more precisely announce the outcomes. Besides, almost all AFs are function in either the experimental voltage $V_{exp}$, the corresponding computed one $V_{com}$, the number of measures datasets $N$, or combination of them.
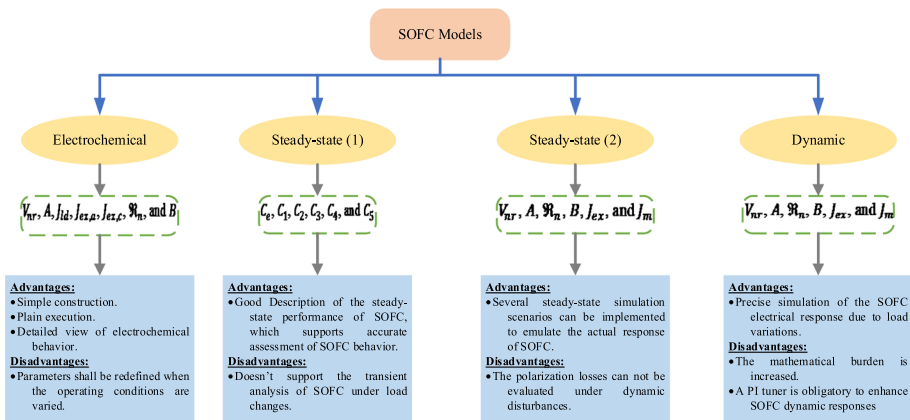


**Fig. 6** Basic Comparison of SOFC models

**Table 2** Brief of practical assessment criteria

| Formula name | Mathematical expression | Characteristics | | Variables | |
| --- | --- | --- | --- | --- | --- |
| | | Absolute | Quadratic | Voltage (V) | Power (W) |
| Absolute deviation (AD) (Chen et al. 2016) | $\left\| V_{exp} - V_{com} \right\|$ | ✓ | | ✓ | |
| Relative absolute deviation (RAD) (Babu et al. 2016) | $\left\| \frac{V_{exp} - V_{com}}{V_{exp}} \right\|$ | ✓ | | ✓ | |
| Mean absolute deviation (MAD) (Sohani et al. 2019) | $\frac{1}{N} \sum_{i=1}^{N} \left\| V_{exp,i} - V_{com,i} \right\|$ | ✓ | | ✓ | |
| Mean quadratic bias deviation (MQBD) (Ayodele et al. 2016) | $\frac{\sum_{i=1}^{N} \left( V_{exp,i} - V_{com,i} \right)^2}{\sum_{i=1}^{N} \left( V_{exp,i} - V_{mean} \right)^2}$ | | ✓ | ✓ | |
| Mean absolute deviation in power (MADP) (Gomes et al. 2016) | $\frac{1}{N} \sum_{i=1}^{N} \left\| P_{exp,i} - P_{com,i} \right\|$ | ✓ | | | ✓ |
| Mean absolute relative deviation (MARD) (Ma et al. 2018) | $\frac{1}{N} \sum_{i=1}^{N} \left\| \frac{V_{exp,i} - V_{com,i}}{V_{exp,i}} \right\|$ | ✓ | | ✓ | |
| Mean quadratic deviation (MQD) (Dai et al. 2011) | $\frac{1}{N} \sum_{i=1}^{N} \left( V_{exp,i} - V_{com,i} \right)^2$ | | ✓ | ✓ | |
| Root mean quadratic deviation (RMQD) (Chen et al. 2019) | $\sqrt{\frac{1}{N} \sum_{i=1}^{N} \left( V_{exp,i} - V_{com,i} \right)^2}$ | | ✓ | ✓ | |
| Normalized root mean quadratic deviation (NRMQD) (Jiang et al. 2019) | $\frac{\sqrt{\frac{1}{N} \sum_{i=1}^{N} \left( V_{exp,i} - V_{com,i} \right)^2}}{V_{exp}}$ | | ✓ | ✓ | |
| Overall quadratic deviation (OQD) (Gouda et al. 2021) | $\sum_{i=1}^{N} \left( V_{exp,i} - V_{com,i} \right)^2$ | | ✓ | ✓ | |

## 4 Meta-Heuristic Optimizers for Parameters Estimation

Over the last two decades, the attention of researchers has been dedicated to MHOs for solving the highly constrained optimization problems (Pan et al. 2023). Most MHOs are population-based algorithms which depend on random initialization of population inside predefined boundaries (Talaat et al. 2023). Moreover, they are considered as iterative approaches in which the solutions get more optimum over the course of iterations (Wang et al. 2020). Based upon the no free launch theorem, there is not a certain optimizer that can solve all the optimization frameworks efficiently. Therefore, electric power systems optimization is still under development to attain the best optimizer for each specific dilemma (Askarzadeh 2017; Kalavani et al. 2019).

MHOs can be mathematically modelled using a set of equations with various forms such as differential, integral, or even algebraic. Furthermore, they can be classified into different techniques based on their operating principles as shown in Fig. 7. In this context, the main classification of MHOs includes evolutionary based, swarm based, physics based, and nature inspired optimizers. However, some reinforcements may be involved in the optimizer structure for better performance. These include but are not limited to better convergence characteristics and obtaining global optimal solution. Eventually, 30 up-to-date MHOs used for SOFC parameters identification will be discussed and investigated regarding basic principles, merits and demerits, limitations, operators, and improvements.
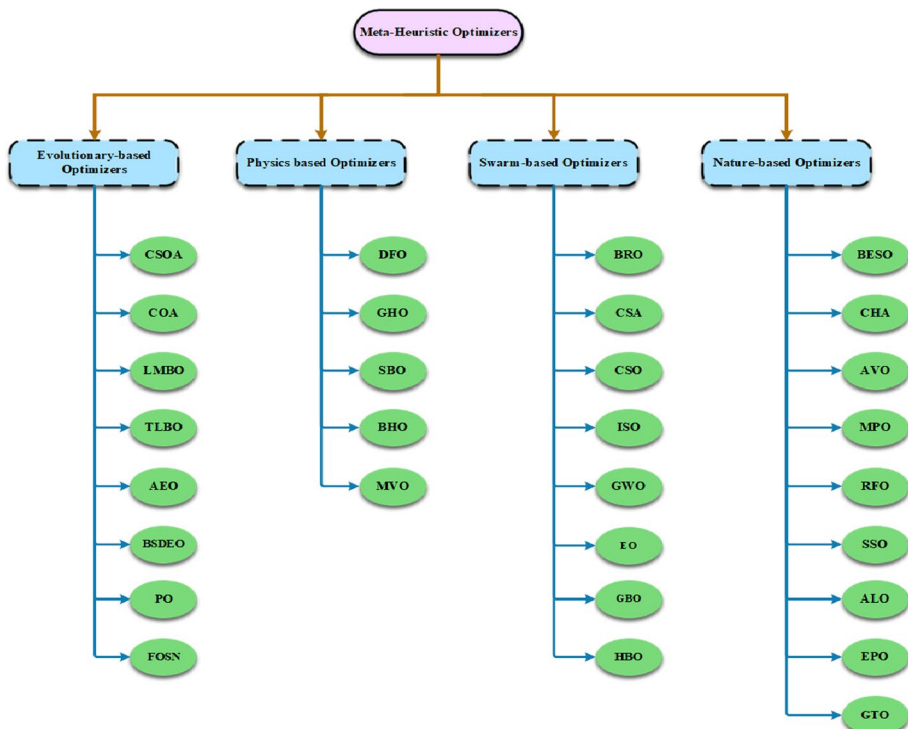


**Fig. 7** Main classifications of MHOs

## 4.1 Evolutionary-Based Optimizers

Such category refers to MHOs that emulate the attitudes of organisms during their living phase. Specifically, they employ biological concepts, like recombination, mutation, and reproduction, related to biological upgrowth.

### 4.1.1 Cooperation Search Optimization Algorithm

The operation of cooperation search optimization algorithm (CSOA) is inspired from the teamwork cooperation inside a company (Feng et al. 2021). Any company may be classified into four categories: members, directors, commanders, and the president. Since the president has the highest authority inside the company, its effect is efficacious while directors and commanders support other members with plentiful advice. Therefore, each solution is represented as a group which can exchange the information with other members such as directors and the president. After the initialization stage, the communication between groups aids in global exploitation phase by exploiting the gained knowledge by group members.

### 4.1.2 Coyote Optimization Algorithm

The coyote optimization algorithm (COA), naturally inspired from coyote's behavior, can be considered as evolutionary-based or swarm-based optimizer implemented for minimization or maximization problems (Zhang et al. 2023). The COA population is divided into packs which in turn consist of a number of coyotes with a maximum value of 14. The social conditions of coyotes are updated through (22) with the aid of their organized interaction and intelligence (Abou El-Ela et al. 2021).

$$SOC_{P,it_{upd}} = SOC_{P,it} + rand1 \times \delta_1 + rand2 \times \delta_2 \tag{22}$$

where $SOC_{P,it_{upd}}$, $SOC_{P,it}$ are the updated and present social condition of the coyote respectively at it$^{th}$ iteration of p$^{th}$ pack. $rand1$, $rand2$ are randomly generated numbers between 0 and 1, while $\alpha c_{P,it}$ denotes the optimal social condition of the coyote.

$$\delta_1 = \alpha c_{P,it} - SOC_{cr1,P,it} \tag{23}$$

$$\delta_2 = Cult_{P,it} - SOC_{cr2,P,it} \tag{24}$$

$\delta_1$ defines the impact difference of a random coyote $cr1$ to the optimal coyote $\alpha c_{P,it}$ at the same pack that is computed from (23). On the other side, $\delta_2$ which is computed from (24) represents the variance of another random coyote $cr2$ to the cultural tendency at the same pack $(Cult_{P,it})$.

### 4.1.3 Levenberg Marquardt Backpropagation Optimizer

Levenberg marquardt backpropagation optimizer (LMBO) can be deemed as a variant of Newton's technique that is appropriate for small size and medium size multilayer networks

(Yang et al. 2021a, b, c). Therefore, the main approach of LMBO can be described as indicated in (25), where in (26) the solution is updated at each iteration (Singla et al. 2019).

$$\Delta x_{it} = -\left[J^T\left(x_{it}\right)J\left(x_{it}\right) + \mu_{it}U\right]^{-1}J^T\left(x_{it}\right)er\left(x_{it}\right) \tag{25}$$

$$x_{it+1} = x_{it} + \Delta x_{it} \tag{26}$$

where $x_{it}, x_{it+1}$ denotes the vector of network parameters in the $it^{th}$ and $(it+1)^{th}$ iteration respectively, $\Delta x_{it}$ represents the variation in network parameters in the $it^{th}$ iteration. In addition, $J\left(x_{it}\right)$ is the Jacobian matrix for the vector $x_{it}$, while $er\left(x_{it}\right)$ defines the vector of errors between the desired output and real output of the network parameters. $U$ designates a unit matrix, while $\mu_{it}$ is a supportive factor for ensuring the efficacy of the inverse matrices.

### 4.1.4 Teaching Learning-Based Optimizer

Teaching learning-based optimizer (TLBO) is a powerful Meta-Heuristic Optimizer (MHO) imitates the classical teaching–learning strategy which forms of two stages: teaching and learning stages (Nama et al. 2020). In the teaching phase, the winning individual is supposed to be the teacher who shares the knowledge to the learners or students as explained in (27) (Pandya and Jariwala 2022).

$$X_{new,it} = X_{old,it} + rand(0, 1) \times \left(X_{teacher} - T_F.X_{mean}\right) \tag{27}$$

where $X_{new,it}, X_{old,it}$ define the new and old positions of the $it^{th}$ learner respectively, $X_{teacher}$ denotes the learners taught from the teacher while $X_{mean}$ is the average position value of all learners. $T_F \in \{1, 2\}$ is the teaching factor that is used to determine the average value to be modified.

In the learning phase, the learning process is still improved where the learners boost their knowledge from the peer-learners. Accordingly, the learning update process can be formulated as mentioned in (28) and (29) where $X_{old,r}$ symbolizes a random learner ($r \neq it$).

$$X_{new,it} = X_{old,it} + rand(0, 1) \times \left(X_{old,it} - X_{old,r}\right), X_{old,it} < f\left(X_{old,r}\right) \tag{28}$$

$$X_{new,it} = X_{old,it} + rand(0, 1) \times \left(X_{old,r} - X_{old,it}\right), X_{old,r} \leq f\left(X_{old,it}\right) \tag{29}$$

However, the classical TLBO suffers from tardy convergence rate which brings out the claim of implementing the ranking based TLBO. In this way, an appropriate equilibrium between exploration and exploitation phases will be fulfilled which in turns accelerates the convergence trend. In this regard, a ranking-based technique is applied for both teachers and learners followed by the pickup probability for each learner. In other words, the higher ranked learner, the larger the selection probability (Ashraf and Malik 2020).

### 4.1.5 Artificial Ecosystem Optimizer

Artificial ecosystem optimizer (AEO) comprises three performance operators starting with the production phase which enhances the exploration and exploitation capabilities. In this stage, AEO producer is considered as the worst agent that shall be updated within defined

lower and upper boundaries. Then, AEO performs its consumption phase where the exploration capability is enhanced. AEO consumer agent obtains the food energy via eating a random low level energy consumer or the producer or both. Accordingly, AEO is terminated with the decomposition phase to promote the exploitation mechanism (Shaheen et al. 2022). However, the conventional AEO may stuck into local minima which brings out the need for enhanced form of AEO by introducing a novel mutation strategy. Consequently, the searching agents will move towards the enriched regions which can be done through implementing gaussian mutation technique as revealed in (30) (El-Dabah et al. 2021).

$$f_{Gaussian} = \frac{e^{\frac{-\alpha^2}{2\sigma^2}}}{\sqrt{2\pi\sigma^2}} \tag{30}$$

where $\alpha$ denotes the linear weight function, $\sigma^2$ is the variance between individuals inside the population.

### 4.1.6 Bernstain Search Differential Evolution Optimizer

Bernstain search differential evolution optimizer (BSDEO) is counted as the developed approach of differential evolution optimizers where each sample vector is evolved separately (Nama and Saha 2020). Therefore, BSDEO is considered as a parallel search optimizer where Bernstain polynomials control the crossover approach. Accordingly, some innovations of BSDEO can be summarized as follows (Civicioglu and Besdok 2019):

- It uses a crossover agent more efficiently than conventional DE optimizers.
- It uses parallel computing techniques.
- It has a flexible rate value of mutation and crossover.
- It is deemed as a partially elitist methodology.

### 4.1.7 Political Optimizer

Political optimizer (PO) is a MHO inspired from the political struggle between two candidates in which each nominee seeks to convince the electors. In PO mechanism, each squad tries to gather the maximum possible number of seats to optimize their goodwill. Therefore, squad members are considered as the candidate solutions while their goodwill is the decision variables to be optimized. PO composes of five consequent stages begin with squad formation, constituencies distribution, electioneering, squad switching, and end with the parliamentary affair stage (Suresh et al. 2021).

The first phase of the PO is executed only once as it expounds the initialization stage of the PO mechanism. On the other side, nominees seek to promote their performance, learn from the former election, and match with the winner in the electioneering phase. Finally, in the last stage, the parliamentarians update their positions based on their calculated fitness value (Mahmoud et al. 2023).

### 4.1.8 Fractional-Order Social Network Optimizer

Naturally, people are social beings who like interacting with others. As a result of the global technological development, social networks have become the trend of

**Table 3** Optimal values of SOFC parameters using evolutionary-based optimizers

| MHO | Test case | Operating conditions | | Parameters' optimal values | | | | | | | | AF $\times 10^{-6}$ |
|---|---|---|---|---|---|---|---|---|---|---|---|---|
| | | $T_{op}$ | $P_H$ | $V_{nr}$ | $A$ | $J_{ex,a}$ | $J_{ex,c}$ | $J_{ex}$ | $J_m$ | $\mathfrak{R}_n$ | $B$ | |
| CSOA (Ismael et al. 2023) | Siemens Energy | 1173 | N.M | 0.8908 | 0.0729 | ✗ | ✗ | 0.0853 | 0.19240 | 0.2531 | 1.0000 | MQD=3.19 |
| COA (Abaza et al. 2020) | 5 kW SOFC | 923 | 3 | 1.1197 | 0.0601 | 0.0180 | 0.0063 | ✗ | 0.15700 | 0.0061 | 0.0535 | MQD=99.91 |
| LMBO (Yang et al. 2021a, b, c) | 5 kW SOFC | 1173 | 1 | 1.0862 | 0.0240 | 0.0207 | 0.0040 | ✗ | 0.15998 | 0.0032 | 0.0736 | RMQD=164.91 |
| TLBO (Xiong et al. 2018) | 5 kW SOFC | 1173 | 1 | 1.0894 | 0.0361 | 0.0275 | 0.0067 | ✗ | 0.15988 | 0.0040 | 0.0653 | MQD=1.53 |
| AEO (Rizk-Allah et al. 2021) | Siemens Energy | 1173 | N.M | 0.8908 | 0.0104 | ✗ | ✗ | 0.0795 | 0.20710 | 0.3880 | 1.1218 | MQD=3.18 |
| BSDEO (Rizk-Allah et al. 2021) | Siemens Energy | 1173 | N.M | 0.8942 | 0.2743 | ✗ | ✗ | 0.0685 | 0.19030 | 0.1327 | 0.7865 | MQD=4.26 |
| PO (Fathy and Rezk 2022) | Siemens Energy | 1073 | N.M | 0.9092 | 0.0109 | ✗ | ✗ | 0.0842 | 1.00000 | 1.0000 | 0.0439 | MQD=2.69 |
| FOSN (Liu et al. 2022) | 5 kW SOFC | 1023 | 3 | 1.1400 | 0.0390 | 0.0224 | 0.0075 | ✗ | 0.15752 | 0.0200 | 0.0660 | OQD=6520 |

\* N.M abbreviates "not mentioned"

communication means. Thus, fractional-order social network optimizer (FOSN) emulates the actions of individuals to achieve wider popularity in the social network. Basically, the interconnection and sharing of ideas among individuals can significantly change one's perspective. So, the individuals' passion to augment their publicity in the social network can be formulated as an optimization problem. Similar to the actual social attitude, the attitude and point of views of individuals in virtual communities also have different phases such as emulation, argument, debate, and innovation (Bayzidi et al. 2021).

Accordingly, each of these phases generates a new solution in FOSN. Specifically, in emulation phase, an individual's perspective attracts the others, where they emulate it in delivering their opinion. Additionally, in the argument stage, individuals talk about diverse ideas and exchange guidance in various cases. Besides, in the debate process, the populations announce their opinions and support their perspectives to persuade others. Finally, the innovation phase happens when individuals share a novel idea or experience in the community (Gnetchejo et al. 2023).

Finally, the numerical results of engaging such optimizers in enhancing the electrical characteristics of SOFCs are captured in Table 3.

## 4.2 Physics-Based Optimizers

The optimization process of such algorithms mainly mimics the physical rules and laws that govern objects' motion, particles' behavior, and gravitational and electromagnetic forces.

### 4.2.1 Dragon Fly Optimizer

Three basic principles have to be fulfilled in dragon fly optimizer (DFO) which are named as separation, alignment, and cohesion (Rahmati and Taherinasab 2023). Separation is performed to avoid the individuals colliding particularly for individuals which are close to each other. Afterwards, alignment is the speed coordination between the individuals and their surroundings while cohesion is the tendency to be located at the bulky center. Nevertheless, DFO requires more adjustments to boost its performance such as utilizing the fractional order DFO. In this way, trapping into local minima is avoided as much as possible (Zhao et al. 2023).

### 4.2.2 Grasshopper Optimizer

In the procedure of Grasshopper optimizer (GHO), the foraging and migration demeanor of grasshopper is arranged for global optimization processes. Accordingly, the general mathematical formula of GHO is presented in (31) mimicking both exploration and exploitation phases (Badr et al. 2023).

$$X_{gi} = S_{gi} + G_{gi} + A_{gi} \tag{31}$$

where $X_{gi}$ defines the position of gi$^{th}$ grasshopper, while $S_{gi}$ denotes the social impact among grasshopper, $G_{gi}$ is the gravity operator of gi$^{th}$ grasshopper, and $A_{gi}$ represents the wind stream flow on the positions of grasshoppers.
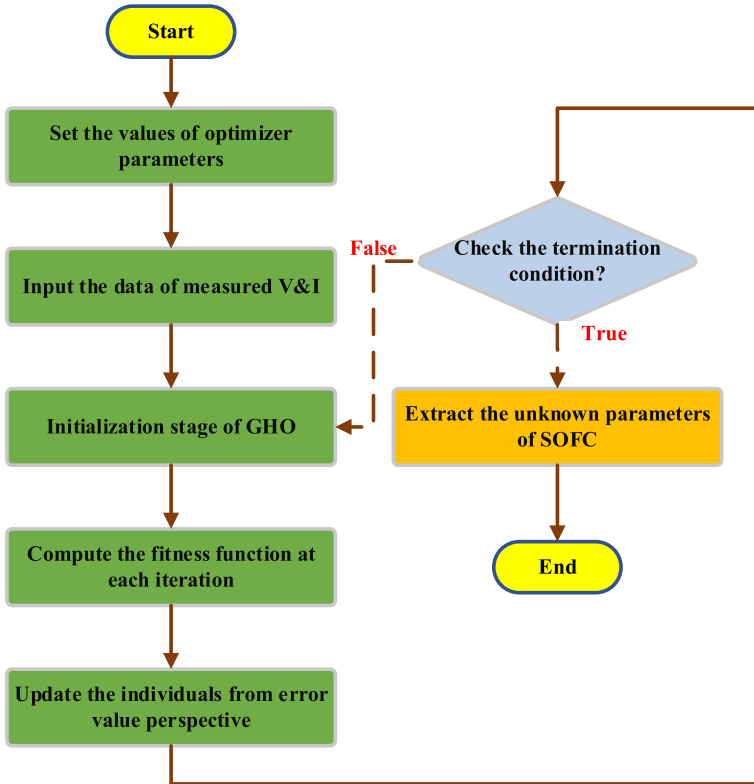
**Fig. 8** Generic flow chart of GHO

As previously mentioned, the position of grasshopper depends on three main factors, although $S_{gi}$ has the major influence among them. It can be described as declared in (32) based on the degree of social influence that occurred (Mirjalili et al. 2018).

$$S_{gi} = \sum_{gj=1}^{Ngrass} s\left(\left|x_{gj} - x_{gi}\right|\right) \frac{x_{gj} - x_{gi}}{\left|x_{gj} - x_{gi}\right|}, \tag{32}$$

where $\left|x_{gj} - x_{gi}\right|$ specifies the distance between the $gi^{th}$ grasshopper and $gj^{th}$ grasshopper where $gi \neq gj$, and *Ngrass* is the total number of grasshoppers. In this context, the general flow chart describing the basic procedure of GHO is illustrated in Fig. 8.

### 4.2.3 Satin Bowerbird Optimizer

Satin bowerbird optimizer (SBO) begins with the generation of uniform random agents containing a group of elected bowers positions. Outspokenly, the generated population shall be bounded between the predefined lower and upper boundaries of the SBO. As in the situation of the most metaheuristic-based optimizers, superior solutions are stored

at each iteration during the optimization procedure. In other words, more experienced males take the attention of others to their bowers. As previously mentioned, the positions of bowers are updated iteratively to converge quickly attaining the best fitness value as declared in (33) (Chintam and Daniel 2018).

$$x_{jb,it}^{new} = x_{jb,it}^{old} + \beta_{it} \left[ \left( \frac{x_{k,it} + x_{elite,it}}{2} \right) - x_{jb,it}^{old} \right] \tag{33}$$

where $x_{jb,it}^{new}, x_{jb,it}^{old}$ are the new and old position of jb$^{th}$ bower at it$^{th}$ iteration respectively, $x_{elite,it}$ is the bower which has the best fitness value that should affect others. $x_{k,it}$ denotes the bower with the large probability, while $\beta_{it}$ is a parameter used to define the step size to pick the target bower that is evaluated from (34) (Duan et al. 2019).

$$\beta_{it} = \frac{\alpha_{it}}{1 + prop_{jb}} \tag{34}$$

where $\alpha_{it}$ defines the charge transfer coefficient, while $prop_{jb}$ is the probability for each jb$^{th}$ bower.

### 4.2.4 Black Hole Optimizer

Black hole optimizer (BHO) is a physics-based algorithm in which a random population is generated and distributed uniformly over the search space. It is worth mentioning that the population evolve in BHO is made by transferring all the candidate individuals towards the best candidate in each iteration (Arenas-Acuña et al. 2021). The best candidate is called the black hole while other candidates are replaced by a new batch of candidates. In other words, BHO can be classified as an updated version of the classical particle optimizer except that the generated particle is usually produced next to the best particle that results in improving the convergence characteristics (Azizipanah-Abarghooee et al. 2014).

### 4.2.5 Multi Verse Optimizer

Multi verse is the opposite term of universe due to the referring of presence more universes rather than the universe we live in. Therefore, the multi verse theory represents the inspiration of multi verse optimizer (MVO) contemplating black holes, white holes, and wormholes. In this context, white and black holes are utilized in the exploration phase of MVO while wormholes are exploited in the exploitation phase. Conversely, the iteration term in MVO is replaced by time to imitate the processes in the multi verse theory (Lakhina et al. 2023).

Furthermore, each individual solution is assigned with an inflation rate to quantify the corresponding fitness value of this solution. The higher the inflation rate, the lower probability of black holes but higher probability of white holes. There are two governing operators in MVO structure: wormhole existence probability (*WEP*) and traveling distance rate (*TDR*) that are computed from (35) and (36) respectively (Amezquita et al. 2023). *WEP* defines the existence probability of wormholes in universes while *TDR* clarifies the distance or variation rate at which the object can be teleported.

**Table 4** Optimal values of SOFC parameters using physics-based optimizers

| MHO | Test case | Operating conditions | | Parameters' optimal values | | | | | | | | AF ×10⁻⁶ |
|---|---|---|---|---|---|---|---|---|---|---|---|---|
| | | $T_{op}$ | $P_H$ | $V_{nr}$ | $A$ | $J_{exa}$ | $J_{exc}$ | $J_{ex}$ | $J_m$ | $\Re_n$ | $B$ | |
| DFO (Guo et al. 2022) | 5 kW SOFC | 837 | 3 | 1.1900 | 0.0600 | 0.0132 | 0.0050 | ✗ | 0.13234 | 0.1261 | 0.0420 | OQD = 228 |
| GHO (Ai et al. 2022) | Siemens Energy | 1173 | N.M | 0.9054 | 0.7404 | ✗ | ✗ | 0.0798 | 0.97180 | 0.7785 | 1.7828 | RMQD = 13.53 |
| SBO (El-Hay et al. 2018) | Siemens Energy | 1173 | N.M | 0.8924 | 0.3457 | ✗ | ✗ | 0.0976 | 0.16290 | 0.2965 | 0.6518 | MQD = 3.41 |
| BHO (Guo et al. 2022) | 5 kW SOFC | 837 | 3 | N.M | N.M | N.M | N.M | ✗ | N.M | N.M | N.M | OQD = 51,900 |
| MVO (Guo et al. 2022) | 5 kW SOFC | 837 | 3 | N.M | N.M | N.M | N.M | ✗ | N.M | N.M | N.M | OQD = 20,800 |

$$WEP = BO_{min} + it \times \left( \frac{BO_{max} - BO_{min}}{IT} \right) \tag{35}$$

$$TDR = 1 - \frac{it^{\frac{1}{\rho}}}{IT^{\frac{1}{\rho}}} \tag{36}$$

where $BO_{min}, BO_{max}$ are the minimum and maximum boundaries respectively, $\rho$ denotes the exploitation precision over the iterations.

To sum up, Table 4 elucidates the optimal values of the SOFC unknown parameters based on the above-mentioned physics-based algorithms.

## 4.3 Swarm-Based Optimizers

Principally, these algorithms employ the collective mechanism of living things for foraging and hunting their prey. Each agent in the swarm has a specific role that serves the group's common goal.

### 4.3.1 Battle Royal Optimizer

Battle royal optimizer (BRO) is a population-based algorithm where the initial population is scattered over the search space. Its operation is inspired from the behavior of the players in a competitive and enduring game such as Call of Duty, and Counter Strike. Initially, all the game competitors are distributed randomly over the game search space that is gradually reduced. Therefore, players should scout for new tools to stay safe in the game that results in one winning player or team. To create a perfect exploration, the location of an injured or killed soldier ($Z_{inj,d}$) with a dimension $d$ is determined through (37) in which its value becomes zero if the soldier can shoot the rival (Samir et al. 2022).

$$Z_{inj,d} = rand_1 \times \left( UB_d - LB_d \right) + LB_d \tag{37}$$

where $LB_d, UB_d$ are lower and upper boundaries of the search space in a dimension $d$ respectively, and $rand_1$ is a random generated number between 0 and 1.

In order to improve the convergence rate and avoid trapping into local minima, two modifications may be applied to the traditional BRO represented in Opposition-Based Learning (OBL) technique or the chaos theory. In the first amendment, each candidate solution can be deemed as a duo of candidates where the location of the duo is supplement of the major candidate. On the other side, chaos theory generates pseudo randomness instead of completely randomness such as a sinusoidal map as explained in (38) (Akan et al. 2022).

$$rand(it + 1)_{c1} = M_c \times rand(it)^2{}_{c1} \times sin\left( \pi \times rand(it)_{c1} \right) \tag{38}$$

where $rand(it + 1)_{c1}, rand(it)_{c1}$ are the random generated chaotic number of the current and previous iteration respectively, and $M_c$ denotes a chaotic controlling parameter.

### 4.3.2 Chameleon Swarm Algorithm

Chameleon swarm algorithm (CSA) imitates the behavior of chameleon in prey hunting in three sequential stages: tracking, searching, and hunting (Ren et al. 2023). As in the case of most metaheuristic optimizers, CSA starts with population initialization followed by the evaluation criterion in which the position's quality is assessed. Afterwards, the peregrination attitude of chameleons through desert and trees tracking for prey is modeled. In the hunting stage, chameleon uses its tongue to catch its prey as fast as possible. Therefore, the speed of chameleon's tongue is mathematically modelled considering the effect of inertia weight ($w1$) which is linearly reduced with the progression of generations as indicated in (39).

$$w1 = \left(1 - \frac{it}{IT}\right)^{\left(\rho 1 \sqrt{\frac{it}{IT}}\right)} \tag{39}$$

where $IT$ defines the maximum number of iterations, and $\rho 1$ denotes a controlling parameter for the exploitation capability. Furthermore, the acceleration rate of chameleon's tongue ($\alpha 1$) can be exponentially modelled as revealed in (40) which $2590 m/s^2$ represents its maximum value.

$$\alpha 1 = 2590 \times \left(1 - e^{-log(it)}\right) \tag{40}$$

It is worth referring that some improvements may be applied to the traditional CSA to prohibit trapping into local minima especially in multi-dimensional problems. This can be achieved by an enhanced searching equation in addition to a novel learning strategy to maintain the track of optimal solutions using the information exchange principle (Zhou and Xu 2023).

### 4.3.3 Competitive Swarm Optimizer

Unlike the traditional particle swarm optimizer (PSO), competitive swarm optimizer (CSO) espouses a pairwise competition as in each iteration the population with $n$ individuals is assigned to $\frac{n}{2}$ pairs alternatively (Xiong and Shi 2018). In this regard, the individual with the minimum fitness function refers to the winner and vice versa. To enhance the effectiveness of the solution, the loser individual learns from the winner one while the winner picks up its progression path towards the upcoming iteration (Cheng and Jin 2014).

### 4.3.4 Interior Search Optimizer

Interior search optimizer (ISO) imitates the design and arrangements of interior places that is inherently supposed as decoration-based simulated optimizer. The only controlling parameter in ISO is $\sigma_i$ which is calculated from (41) implements the detachment between mirror and composition groups (Rizk-Allah et al. 2023). As it is declared in (41), the value of $\sigma_i$ is updated in each iteration without any involvement from the user.
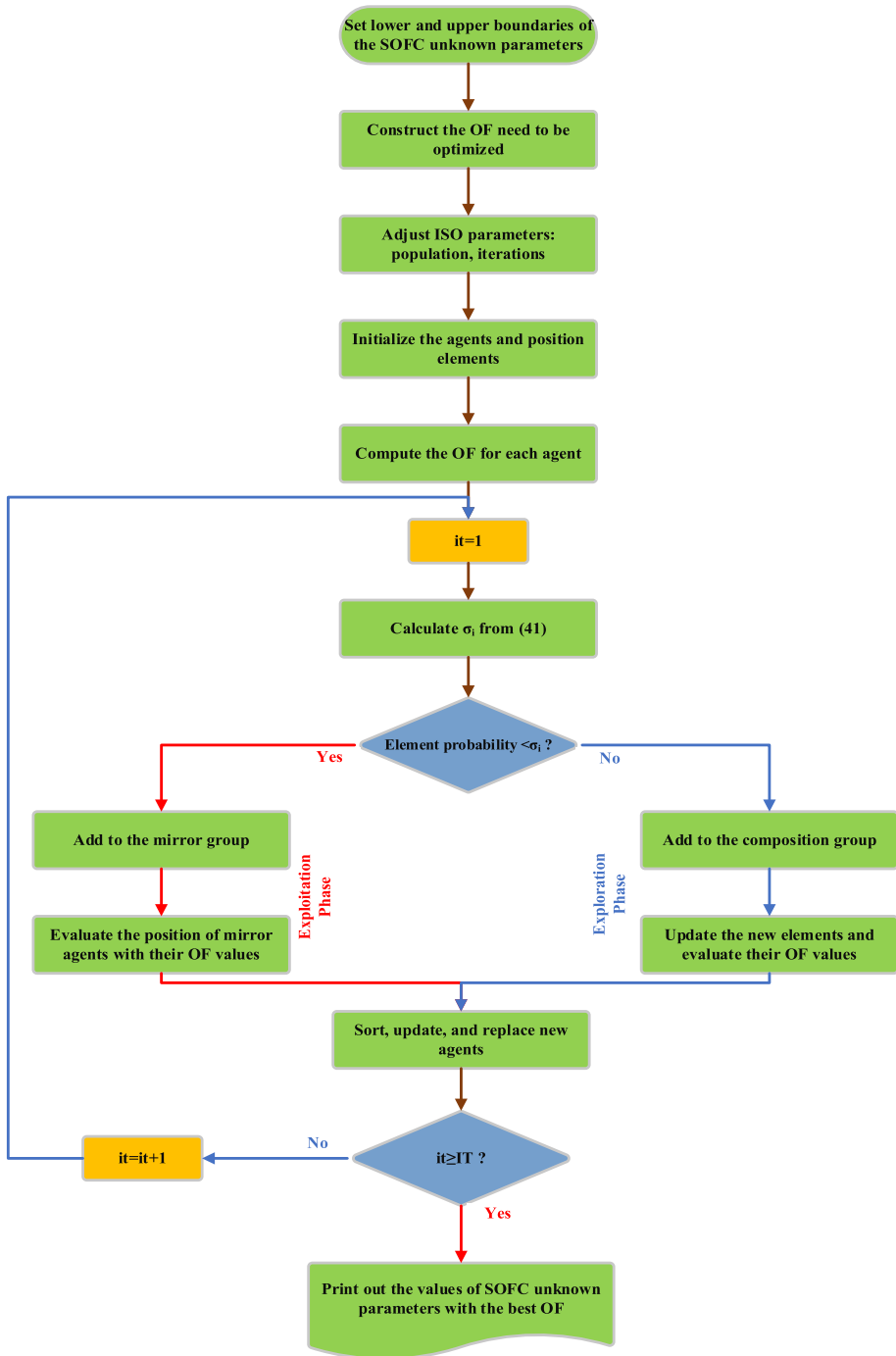
$$\sigma_i = \frac{it}{IT} \tag{41}$$

**Fig. 9** Generic procedure of ISO

```
                        ┌──────────┐
                        │  Start   │
                        └────┬─────┘
                             ▼
              ┌─────────────────────────────────┐
              │ Set up the optimizer parameters  │
              └─────────────────┬───────────────┘
                                ▼
          ┌───────────────────────────────────────────┐
          │ Input population and maximum iterations size │
          └───────────────────┬───────────────────────┘
                              ▼
          ┌───────────────────────────────────────────┐
          │ Initialize the search agents of ACGWO        │
          └───────────────────┬───────────────────────┘
                              ▼
          ┌───────────────────────────────────────────┐
          │ Evaluate the fitness function for each      │
          │ individual                                  │
          └───────────────────┬───────────────────────┘
                              ▼
          ┌───────────────────────────────────────────┐
          │ Update the chaotic sequence of chaotic map  │
          └───────────────────┬───────────────────────┘
                              ▼
          ┌───────────────────────────────────────────┐
          │ Update the position of wolves and recalculate│
          │ the fitness values                          │
          └───────────────────┬───────────────────────┘
                              ▼
          ┌───────────────────────────────────────────┐
          │ Proceed to another iteration and then compute│
          │ the value of the improved convergence factor │
          │ from (42)                                    │
          └───────────────────┬───────────────────────┘
                              ▼
                    ◇ Check the termination condition? ◇ ── NO ──┐ (loop back)
                              │ YES
                              ▼
          ┌───────────────────────────────────────────┐
          │ Update the wolves positions                 │
          └───────────────────┬───────────────────────┘
                              ▼
                        ┌──────────┐
                        │  Stop    │
                        └──────────┘
```
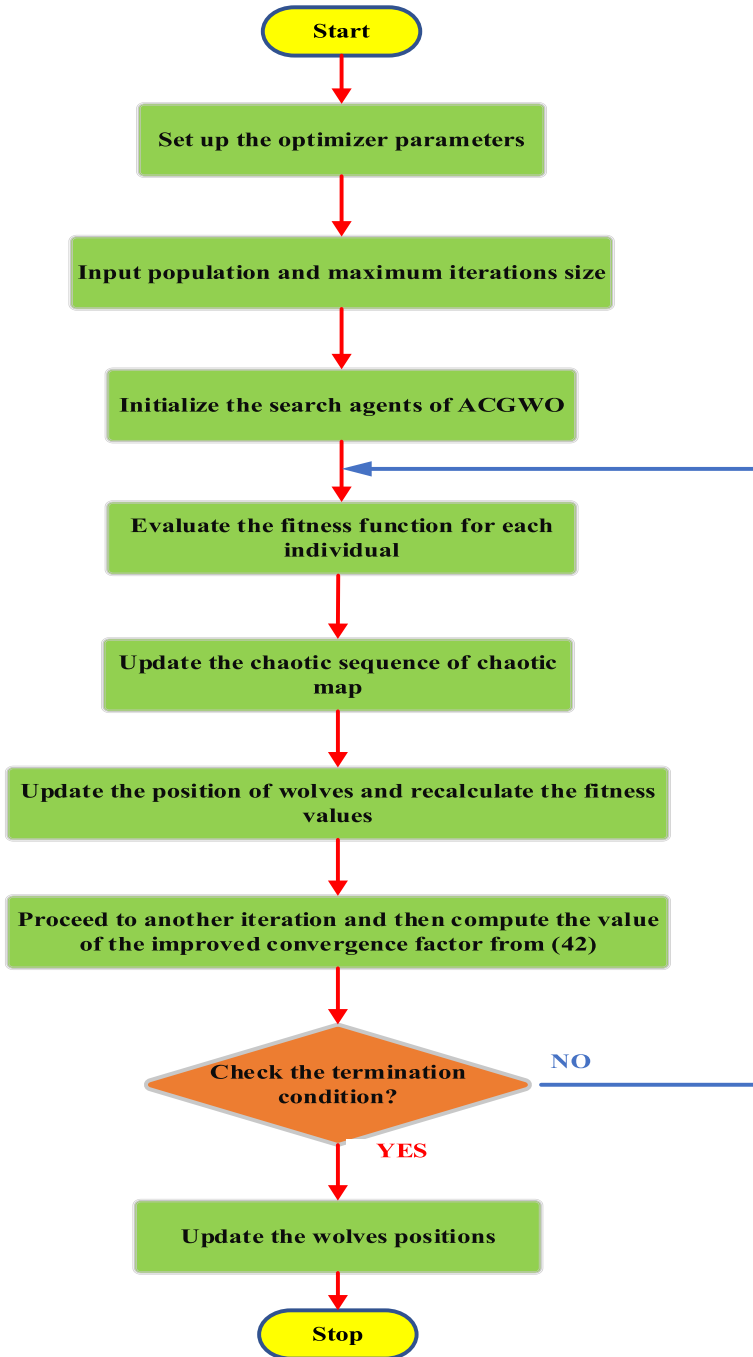
**Fig. 10** Adaptive Chaotic GWO flowchart

where *it* denotes the current iteration of ISO, and *IT* defines the maximum value of executed iterations. It is worth mentioning that the value of $\sigma_i$ is bounded between 0 and 1 while Fig. 9 depicts the general procedure of ISO (Fathy and Rezk 2020).

### 4.3.5 Grey Wolf Optimizer

Grey wolf optimizer (GWO) is a benchmark MHO for solving complicated optimization problems which imitates the hunting approach of wolves to small animals. Basically, the GWO mechanism comprises four layers where the first three layers manage the search and hunting processes while the last one ensures safety in completing the predation. Hereinafter, adaptive chaotic version of GWO outperforms the traditional technique for attaining fast conversion while preserving the diversity of population. Moreover, chaos randomness in the exploration phase helps to dodge trapping into local minima (Hatta et al. 2019).

For the sake of proper coordination between exploration and exploitation capabilities, an improved convergence factor is introduced in GWO structure. This balance can accomplish the trade-off mechanism when non-linear convergence factor is exploited ($a_{GW}$) as presented in (42). For simplicity, Fig. 10 depicts the flow chart of the principles for adaptive chaotic GWO (Elsisi 2022).

$$a_{GW} = 2 - 2 * \left[ \left( \frac{1}{e-1} \right) \times \left( exp\left( \frac{it}{IT} \right) - 1 \right) \right] \tag{42}$$

### 4.3.6 Equilibrium Optimizer

The mass balance equation is a revelation of developing the equilibrium optimizer (EO) in which three determinants are used for the updating processes of particles (Zhang and Lin 2022). The first one is the equilibrium concentration which is implemented to be the selection strategy. The concentration variance between the balance state and each particle is the second term which acts as the dynamic search technique. The third operator deals with the random generation mechanism at which the solution is redefined. In addition, EO has the advantage of employing a memory-based mechanism that supports each particle to track its best coordinates in the space at each iteration. This approach assists to enhances the exploitation abilities by overwriting the later fitness value with an updated better one.
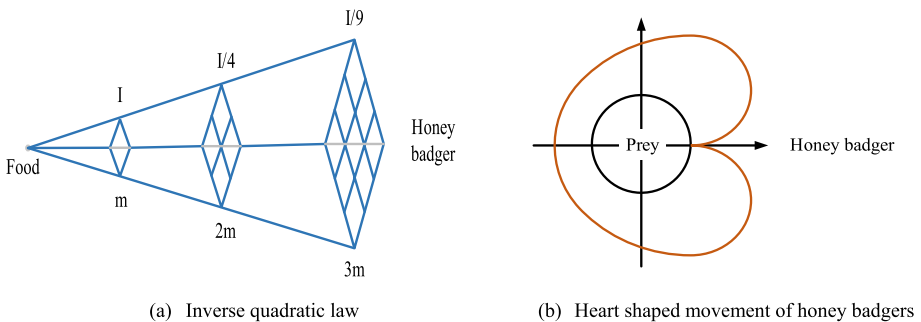


(a) Inverse quadratic law    (b) Heart shaped movement of honey badgers

**Fig. 11** Honey badger tactics

**Table 5** Optimal values of SOFC parameters using swarm-based optimizers

| MHO | Test case | Operating conditions | | Parameters' optimal values | | | | | | | | AF $\times 10^{-6}$ |
|---|---|---|---|---|---|---|---|---|---|---|---|---|
| | | $T_{op}$ | $P_H$ | $V_{nr}$ | $A$ | $J_{ex,a}$ | $J_{ex,c}$ | $J_{ex}$ | $J_m$ | $\mathfrak{R}_n$ | $B$ | |
| BRO (Karamnejadi Azar et al. 2022) | 5 kW SOFC | 1023 | 3 | 1.2800 | 0.0510 | 0.0244 | 0.0075 | | 0.1673 | 0.0050 | 0.0770 | MQD = 3970 |
| CSA (Rizk-Allah et al. 2021) | Siemens Energy | 1073 | N.M | 0.9337 | 1.7217 | ✗ | ✗ | 0.0897 | 0.9851 | 0.3919 | 2.1782 | MQD = 6.6232 |
| CSO (Xiong et al. 2020) | Siemens Energy | 1073 | N.M | 0.9254 | 0.0124 | 0.1000 | 0.1000 | ✗ | 0.9452 | 0.0010 | 0.4195 | MQD = 2.9215 |
| ISO (El-Hay et al. 2019) | Siemens Energy | 1073 | N.M | 0.9279 | 0.5822 | ✗ | ✗ | 0.0299 | 0.5040 | 0.7133 | 0.6024 | MQD = 3.4273 |
| GWO (Hao and Sobhani 2021) | 5 kW SOFC | 1073 | 5 | 1.1498 | 0.0292 | 0.0265 | 0.0034 | ✗ | 0.1552 | 0.0045 | 0.0672 | MQD = 0.3564 |
| EO (Rizk-Allah et al. 2021) | Siemens Energy | 1073 | N.M | 0.9301 | 2.1454 | ✗ | ✗ | 0.0996 | 0.8604 | 0.1496 | 1.0278 | MQD = 3.6575 |
| GBO (Rizk-Allah et al. 2021) | Siemens Energy | 1073 | N.M | 0.9303 | 2.1570 | ✗ | ✗ | 0.0992 | 1.0000 | 0.3244 | 0.9362 | MQD = 3.6577 |
| HBO (Yakout et al. 2022) | Siemens Energy | 1073 | N.M | 0.9074 | 0.0107 | ✗ | ✗ | 0.0997 | 1.0000 | 1.0000 | 0.0441 | MQD = 2.6900 |

### 4.3.7 Gradient-Based Optimizer

Gradient-based optimizer (GBO) is a mixed optimizer between gradient and non-gradient based techniques. Gradient-based methods such as Newton's methos while the other form belongs to most MHOs. It combines the principles of both types to attain a feasible balance between exploration and exploitation phases. Furthermore, GBO has two main controllers: gradient search operator and local escape operator. The first controller promotes the convergence rate by enhancing the exploration mechanism while the second one prevents GBO from being trapped into local minima. GBO proves its superiority in finding the global optimal solutions even in the high dimensional optimization problems (Daoud et al. 2023).

### 4.3.8 Honey Badger Optimizer

Mainly, honey badger optimizer (HBO) imitates the smart behavior of honey badgers while looking for their prey. To locate their food, honey badgers apply two approaches. Firstly, they rely on their smell sense to detect the food location and then begin digging to grab the bee honey. Secondly, they walk through the instructions of the honeyguide bird to locate the beehive. Particularly, HBO involves the two phases (digging and honey) that denote its exploration and exploitation stages (Fathy et al. 2023).

After initializing the population, the smell intensity of honey badgers $I_s(i)$ to the food is defined according to Inverse Square Law, as graphed in Fig. 11a. During the digging phase, the badgers move in a cardioid shape, as revealed in Fig. 11b (Chang et al. 2023).

Lastly, the reader is encouraged to browse Table 5 for further information about the outcomes of the swarm-based optimizers in SOFC parameters determination.

## 4.4 Natural-Based Optimizers

Mainly, these approaches emulate the natural phenomena occurring whether environmentally, animally, or spatially.
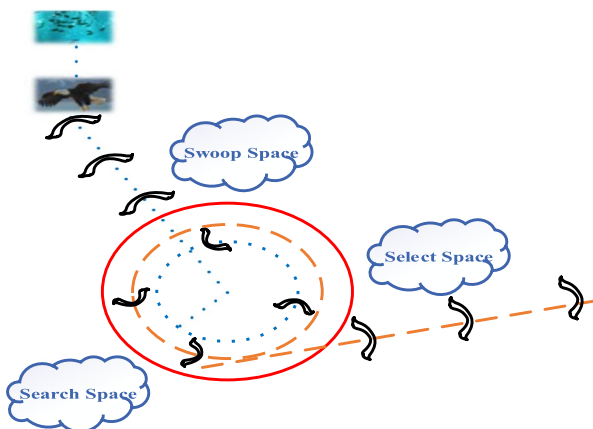


**Fig. 12** BESO hunting stages

### 4.4.1 Bald Eagle Search Optimizer

Bald eagle search optimizer (BESO) is a new metaheuristic nature inspired algorithm with an inspired imitation from the hunting behavior of eagles to the fishes as shown in Fig. 12. It passes through three consecutive hunting stages initialized by the select stage then the search stage and ended by the swooping stage (Rezk et al. 2023).

(a) *Select Stage*

In this phase, eagles select the best hunting search area that contains the majority of fishes in the whole search space. This stage is explained in (43) by defining the updated hunting position $\left(O_{it,upd}\right)$ by knowing the best hunting position from the last iteration $\left(O_{best}\right)$.

$$O_{it,upd} = O_{best} + \alpha_2 \times rand_2\left(O_{avg} - O_{it}\right) \tag{43}$$

where $\alpha_2$ is a controlling parameter with a value confined between 1.5 and 2, while $rand_2$ is a randomness factor between 0 and 1. $O_{it}$ denotes the it$^{\text{th}}$ iteration position, while $O_{avg}$ denotes the average position of the previous information in search areas.

(b) *Search Stage*

In this stage, eagles, with the aid of helix movements, start to recognize the superior position for prey hunting as illustrated in (44).

$$O_{it,upd} = O_{it} + y_1(it) \times \left(O_{it} - O_{it+1}\right) + x_1(it) \times \left(O_{avg} - O_{it}\right) \tag{44}$$

where $O_{it+1}$ is the updated position from the next iteration, while $x_1(it)$ and $y_1(it)$ have predefined formulas which can be found in (Fathy 2023).

(c) *Swooping Stage*

In the swooping stage, eagles rapidly start the hunting action from the best predetermined point by updating the position of all points as illustrated in (45).

$$O_{it,upd} = rand_3 \times O_{best} + x_2(it) \times \left(O_{it} - f_1 \times O_{avg}\right) + y_2(it) \times \left(O_{it} - f_2 \times O_{best}\right) \tag{45}$$

where $rand_3$ is a randomness factor between 0 and 1, $f_1$ and $f_2$ are controlling parameters aid in the speedy movement of eagles, while $x_2(it)$ and $y_2(it)$ have predefined formulas which can be found in (Fathy 2023).

### 4.4.2 Cat Hunting Algorithm

The optimization methodology is mathematically modelled using cat hunting algorithm (CHA) inspired from the fascinating attitude of cats in hunting (Ghaedi et al. 2023). CHA is split into two stages: searching and tracking for prey and revealing or moving towards the target. In this context, each cat has specified abilities in which the more experience the cat has the more it contains the optimal solution. Furthermore, the conventional CHA can

be boosted using OBL technique to enhance the exploration phase of the metaheuristics as revealed in (46).

$$X\_CH, new = X_{CH,max} + X_{CH,min} - X_{CH,new} \tag{46}$$

where $X\_CH, new$ symbolizes the reverse position of the cat's position $X_{CH,new}$, while $X_{CH,min}, X_{CH,max}$ represent the lower and upper limits of the solution respectively.

### 4.4.3 African Vulture Optimizer

African vulture optimizer (AVO) is a metaheuristic algorithm inspired form the natural hunting behavior of vultures which are considered as type of bird originated in most of the world's regions. Vultures feed on the carcasses of living things which may be filled with infections such as anthrax that can kill any creature. However, these maladies cannot harm vultures which aid to immaculate the earth from such harmful diseases. In this regard, a tough fight has broken out between vultures seeking food when they find the food's origin. For this reason, weak vultures follow strong ones and surround them until they get tired in which this process is mathematically modelled. First, the initialization stage of AVO is carried out setting up the values of population and maximum iterations. Then, the starvation rate of vultures is computed from (47) and (48) where vultures fly at high altitudes catching their food when the energy is expired (Mohammed et al. 2023).

$$q_{sub} = k_{AV} \times \left( sin^{\gamma} \left( \frac{\pi}{2} \times \frac{it}{IT} \right) + cos \left( \frac{\pi}{2} \times \frac{it}{IT} \right) - 1 \right) \tag{47}$$

$$H_{AV} = \left( 2 \times \beta + p_{av} \right) \times y_{av} \times \left( 1 - \frac{it}{IT} \right) + q_{sub} \tag{48}$$

where $k_{AV}$ is a random number with a domain of $[-2, 2]$, $\gamma$ defines a set fixed number which recognizes the operational phases, $\beta$, $y_{av}$, and $p_{av}$ symbolize random numbers between 0 and 1.

However, an enhanced version of AVO relies on the collective guidance factor technique may be exploited. In this way, the convergence rate of the optimizer will be boosted defining location and direction for each candidate solution (Fahmy et al. 2023).

### 4.4.4 Marine Predator Optimizer

Marine predator optimizer (MPO) stimulus is motivated from the behavior of predators in attacking their prey and searching for food source (Abdel-Basset et al. 2022). MPO kicks off with the traditional initialization stage between the defined lower and upper boundaries for each predator and prey. MPO agents are defined using two metrices: elite and best metrices which involve the best predators and prey positions. MPO-based methodology is organized form three phases which can be summarized as follows (Al-Betar et al. 2023):

(a)  *High Speed Motion*

It is also named as the exploration phase where the optimizer discloses the search space and assigned the initial third of iterations for this stage. In this phase, predators pause movements while prey proceed quicky towards the food origin.

(b)  *Unit Speed Ratio*

It is also named as the transition phase in which the smooth transformation between exploration and exploitation phases occurs. Moreover, both predators and prey move with the same velocity searching for the food source. Meanwhile, a dominant parameter in MPO methodology (*CF*) which is calculated from (49) controls the step size of predator's transmission.

$$CF = \left(1 - \frac{it}{IT}\right)^{2\frac{it}{IT}} \tag{49}$$

(c)  *Low Speed Ratio*

It is also named as the exploitation phase where agents utilize the optimal solution for smooth convergence rate. Simplicity, the last third of MPO iterations is assigned to the intensification stage where the predator moves quickly towards the prey.

### 4.4.5  Red Fox Optimizer

Red fox optimizer (RFO) principles are inspired from the behavior of red foxes which are characterized by intelligence, adaptability, and high speed (Połap and Woźniak 2021). The hunting mechanism is assisted by the approach of slowly attacking the bait while hiding in the trees. Consequently, the first stage of RFO is the exploration where foxes select their baits from long distances and then the exploitation phase in which foxes' approach to the bait is simulated. At the end of the algorithm, the worst candidates are eliminated and replaced by others causing regeneration of the alpha couple.

Nevertheless, of the RFO merits, it may suffer from trapping into local minimal or precocious convergence. For that reason, some amendments can be introduced such as using Quasi oppositional or chaotic concept techniques.

### 4.4.6  Shark Smell Optimizer

Shark smell optimizer (SSO) simulates the smelling sense of sharks in hunting their prey when there is a notable rise in blood odor concentration (Han et al. 2023). SSO starts with initializing the population expressed in sharks' positions and then attacking the prey is mathematically modelled. The movement of sharks towards baits takes the form of forward and rotational motion although the speed has limitations in the optimizer structure. However, the traditional SSO can be promoted using the chaotic approach depending on the logistic map that will boost its exploration abilities. Moreover, another developed version of SSO is the binary SSO by integrating binary integer individuals. Consequently, suitable transformation format of these binary variables in the search agents can be fulfilled in rotational and forward motion directions (Rao et al. 2019).

### 4.4.7  Ant Lion Optimizer

Ant lion optimizer (ALO) imitates the hunting manner of ant lions such that their lifestyle is modelled in ALO structure like random walk, snaring ants in the pits, and constructing new pits. Because of random walk of ants in every simulated time step, their positions are

**Fig. 13** Huddling attitude of emperor penguins
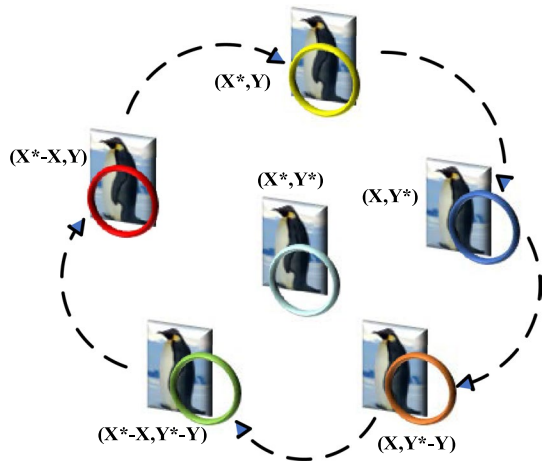


updated iteratively in the search space. Consequently, the position of each ant lion ($X_j^{it}$) can be normalized as expressed in (50) (Azizi et al. 2020).

$$X_j^{it} = \frac{\left(X_j^{it} - a_j\right) \times \left(d_j^{it} - c_j^{it}\right)}{\left(b_j - a_j\right)} + c_j \tag{50}$$

where $a_j, b_j$ are lower and upper limits of the random walk feature for j[th] ant respectively, while $c_j^{it}, d_j^{it}$ define minimum and maximum limits of the jth decision variables in it[th] iteration respectively.

ALO performance can be enhanced using the elitism phenomenon where the convergence trend becomes faster. The new position of jth ant ($ant_j^{it}$) can be evaluated using the average value of two walks as described in (51) (Zeghdi et al. 2022).

$$ant_j^{it} = \frac{R_a^{it} + R_e^{it}}{2} \tag{51}$$

where $R_a^{it}$ defines the ant's movement in roulette wheel, while $R_e^{it}$ defines the elite ant lion in the it[th] iteration.

### 4.4.8 Emperor Penguin Optimizer

Emperor penguin optimizer (EPO) is a bio-inspired MHO that imitates the living behavior of emperor penguins in which the huddling attitude is mathematically modelled. As it is declared in Fig. 13, the huddle behavior is assumed to be on a polygon plane of L-shape where the objective is to find the best mover. EPO starts with the random initialization of the huddle boundaries followed by temperature profile assessment near the huddle. Afterwards, the space between emperor penguins is evaluated to complete exploration and exploitation portfolios. Finally, the optimal solution is selected as the best mover among all emperor penguins which is used to recalculate the boundaries for the updating process (Khalid et al. 2023).

**Table 6** Optimal values of SOFC parameters using nature-based optimizers

| MHO | Test case | Operating conditions | | Parameters' optimal values | | | | | | | | | $AF \times 10^{-6}$ |
|---|---|---|---|---|---|---|---|---|---|---|---|---|---|
| | | $T_{op}$ | $P_H$ | $V_{nr}$ | $A$ | $J_{ex,a}$ | $J_{ex,c}$ | $J_{ex}$ | $J_m$ | $\mathfrak{R}_n$ | $B$ | | |
| BESO (Abaza et al. 2022) | 5 kW SOFC | 923 | 3 | 1.1196 | 0.0596 | 0.0175 | 0.0062 | ✗ | 0.1569 | 0.0061 | 0.0527 | | MQD=0.00002362 |
| CHA (Kele et al. 2022) | 5 kW SOFC | 953 | 5 | 1.3520 | 0.0430 | 0.0281 | 0.0072 | ✗ | 0.1615 | 0.0160 | 0.0870 | | MQD=1150 |
| AVO (Bagal et al. 2021) | 5 kW SOFC | 837 | 3 | 1.3100 | 0.0690 | 0.0158 | 0.0072 | ✗ | 0.1533 | 0.1000 | 0.0520 | | MQD=26.40 |
| MPO (Yousri et al. 2021) | 100 kW SOFC | 1273 | N.M | 1.2000 | 0.0489 | ✗ | ✗ | 0.0974 | 0.8701 | $0.3 \times 10^{-5}$ | 0.1628 | | MQD=3.38 |
| RFO (Luo & Shafiee 2021) | 5 kW SOFC | 837 | 3 | 1.3200 | 0.0960 | 0.0157 | 0.0068 | ✗ | 0.1513 | 0.1200 | 0.0480 | | MQD=6.34 |
| SSO (Wei & Stanford 2019) | Siemens Energy | 1213 | 3 | 0.8471 | 0.0005 | ✗ | ✗ | 0.0290 | 0.1351 | 0.2057 | 0.5179 | | MQD=8.14 |
| EPO (Guo et al. 2022) | 5 kW SOFC | 837 | 3 | N.M | N.M | N.M | N.M | ✗ | N.M | N.M | N.M | | OQD=3960 |
| GTO (Yakout et al. 2022) | Siemens Energy | 1073 | N.M | 0.9182 | 0.0107 | ✗ | ✗ | 0.0362 | 1.0000 | 1.0000 | 0.0441 | | MQD=2.69 |

### 4.4.9 Gorilla Troop Optimizer

Gorilla troop optimizer (GTO) is a new nature-inspired optimizer imitates the attitude of gorillas for hunting exploring for the food (Shaheen et al. 2023a, b). The silverback gorilla is considered as the alpha male of the group which heads their hunting process. Contrarily, the weakest gorilla among the group is deemed as the worst solution that will be ignored in next iterations. Consequently, other gorillas seek to move away from the worst gorilla and approach more to the silverback candidate. In GTO exploration phase, three diverse techniques are represented by the migration of gorillas either in unknown or known location and movement of other gorillas. In the exploitation phase, two techniques are implemented: following for the alpha male gorilla and the other is a competition for the alpha female (Shaheen et al. 2023a, b).

It's time now to check how efficient nature-based algorithms are in allocating the undefined parameters of SOFCs, as revealed in Table 6.

## 5 Illustrative Discussions

In this section, a comprehensive discussion is implemented regarding the computational setting of MHOs and their corresponding studied SOFC's test cases along with their operating conditions. Moreover, a fair and accurate statistical assessment of MHOs' outcomes in SOFC parameter specification is also included.

### 5.1 Numerical and Statistical Evaluation

For a better understanding of the numerous earlier-discussed MHOs, the reader is invited to check the extensive summary presented in Table 7. Particularly, it offers a comprehensive overview of the MHOs in terms of their settings and details of their corresponding SOFC test cases. In other words, regarding MHO settings, Table 7 contains the year of publication, tuned parameters, number of intended executions, and types of statistical evaluations. On the other side, regarding SOFC test cases, it includes model type, number of ungiven parameters, assessment criteria, type of simulated curves, simulations in different conditions, and finally, studied test cases.

Furthermore, Fig. 14a–c reveal a graphical comparison among the achievements of diverse MHOs, in terms of best and average fitness, and standard deviation values, respectively. It's worth stating that all the optimizers, depicted in Fig. 14, are assessed under same test case (5 kW SOFCs stack), same operating conditions ($T_{op} = 1173K$), and identical assessment formula (MQD) to ensure fair judgment. On the other side, Fig. 14d ranks these MHOs based on their computational effort, in terms of the elapsed time per single independent run and the smoothness of the convergence trend. It's worth noting that only nine MHOs are captured in Fig. 14d since those are all implemented in identical operating system specifications (Windows version, RAM, and processor), to guarantee a fair comparison.

A closer look at Fig. 14, the reader can notice that CSO outperforms the other MHOs when considering minimum attainable objective function (MQD), while SSO takes the lead statistically in terms of minimum standard deviation. This is not a surprise, as according to "no free lunch" (NFL) theorem, each optimization method has its own

**Table 7** Comprehensive summary of MHOs for SOFC parameter estimation

| Family | Optimizer | Year | $N_{un}$ | AF | Tuned parameters' | | | $N_{IE}$ | Model | Simulated curves | | | Different conditions | | Statistical assessment | | Test cases |
|---|---|---|---|---|---|---|---|---|---|---|---|---|---|---|---|---|---|
| | | | | | IT | $N_p$ | others | | | V-I | P-I | I-t & V-t | $P_H$ | $T_{op}$ | Parametric | Non-parametric | |
| Evolutionary | CSOA (Ismael et al. 2023) | 2023 | 6 | MQD | 100 | 25 | 1 | 100 | Steady-state (2) | ✓ | ✓ | ✗ | ✗ | ✓ | ✓ | ✓ | Siemens Energy SOFC |
| | | | | | | | | | Dynamic | ✗ | ✗ | ✓ | ✗ | ✗ | ✗ | ✗ | 100 kW SOFC |
| | COA (Abaza et al. 2020) | 2020 | 7 | MQD | 250 | N.M | 2 | N.M | Electrochemical | ✓ | ✓ | ✗ | ✗ | ✓ | ✗ | ✗ | 5 kW SOFC |
| | LMBO (Yang et al. 2021a, b, c) | 2021 | 7 | RMQD | 200 | 50 | 2 | 20 | Electrochemical | ✗ | ✗ | ✗ | ✓ | ✓ | ✗ | ✓ | 5 kW SOFC |
| | | | 6 | | | | | | Steady-state (2) | ✗ | ✗ | ✗ | ✓ | ✓ | ✗ | ✓ | 5 kW SOFC |
| | TLBO (Xiong et al. 2018) | 2018 | 7 | MQD | 50,000 | 40 | 2 | 50 | Electrochemical | ✓ | ✓ | ✗ | ✓ | ✓ | ✗ | ✓ | 5 kW SOFC |
| | AEO (Rizk-Allah et al. 2021) | 2021 | 6 | MQD | 100 | 50 | 1 | 20 | Steady-state (2) | ✗ | ✗ | ✗ | ✗ | ✗ | ✓ | ✓ | Siemens Energy SOFC |
| | | | | | | | | | | ✗ | ✗ | ✗ | ✗ | ✗ | ✓ | ✓ | 5 kW SOFC |
| | BSDEO (Rizk-Allah et al. 2021) | 2021 | 6 | MQD | 100 | 50 | 1 | 20 | Steady-state (2) | ✗ | ✗ | ✗ | ✗ | ✗ | ✓ | ✓ | Siemens Energy SOFC |
| | | | | | | | | | | ✗ | ✗ | ✗ | ✗ | ✗ | ✓ | ✓ | 5 kW SOFC |
| | PO (Fathy & Rezk 2022) | 2022 | 6 | MQD | 100 | 50 | 1 | 50 | Steady-state (2) | ✓ | ✓ | ✗ | ✓ | ✓ | ✗ | ✓ | Siemens Energy SOFC |
| | | | | | | | | | Steady-state (2) | ✓ | ✓ | ✗ | ✗ | ✓ | ✗ | ✗ | 5 kW SOFC |
| | | | | | | | | | Steady-state (2) | ✗ | ✗ | ✗ | ✗ | ✗ | ✗ | ✗ | 100 kW SOFC |
| | | | | | | | | | Dynamic | ✓ | ✓ | ✓ | ✓ | ✓ | ✓ | ✗ | 100 kW SOFC |
| | FOSN (Liu et al. 2022) | 2022 | 7 | OQD | 300 | 40 | ✗ | 35 | Electrochemical | ✓ | ✓ | ✗ | ✓ | ✓ | ✓ | ✗ | 5 kW SOFC |

**Table 7** (continued)

| Family | Optimizer | Year | $N_{un}$ | AF | Tuned parameters' IT | Tuned parameters' $N_p$ | Tuned parameters' others | $N_{IE}$ | Model | Simulated curves V-I | Simulated curves P-I | Simulated curves I-t & V-t | Different conditions $P_H$ | Different conditions $T_{op}$ | Statistical assessment Parametric | Statistical assessment Non-parametric | Test cases |
|---|---|---|---|---|---|---|---|---|---|---|---|---|---|---|---|---|---|
| Physics | DFO (Guo et al. 2022) | 2022 | 7 | OQD | 200 | 120 | 1 | 30 | Electrochemical | ✓ | ✓ | ✗ | ✓ | ✓ | ✗ | ✗ | 5 kW SOFC |
| | GHO (Ai et al. 2022) | 2018 | 6 | MQD | 100 | 50 | 5 | 20 | Steady-state (2) | ✗ | ✗ | ✗ | ✗ | ✗ | ✓ | ✓ | Siemens Energy SOFC |
| | | | | | | | | | Steady-state (2) | ✗ | ✗ | ✗ | ✗ | ✗ | ✓ | ✓ | 5 kW SOFC |
| | SBO (El-Hay et al. 2018) | 2018 | 6 | MQD | 100 | 50 | 3 | 20 | Steady-state (2) | ✓ | ✓ | ✗ | ✗ | ✓ | ✓ | ✓ | Siemens Energy SOFC |
| | | | | | | 60 | | | Steady-state (2) | ✓ | ✓ | ✗ | ✗ | ✗ | ✓ | ✓ | 5 kW SOFC |
| | | | | | | 60 | | | Dynamic | ✓ | ✓ | ✓ | ✗ | ✗ | ✗ | ✗ | 100 kW SOFC |
| | BHO (Guo et al. 2022) | 2022 | 7 | OQD | 200 | 120 | 2 | 30 | Electrochemical | ✓ | ✓ | ✗ | ✓ | ✓ | ✗ | ✗ | 5 kW SOFC |
| | MVO (Guo et al. 2022) | 2022 | 7 | OQD | 200 | 120 | 2 | 30 | Electrochemical | ✓ | ✓ | ✗ | ✓ | ✓ | ✗ | ✗ | 5 kW SOFC |
| | BRO (Karamnejadi Azar et al. 2022) | 2022 | 7 | MQD | 200 | 50 | 2 | 25 | Electrochemical | ✓ | ✓ | ✗ | ✓ | ✓ | ✓ | ✓ | 5 kW SOFC |
| Swarm | CSA (Rizk-Allah et al. 2021) | 2021 | 6 | MQD | 100 | 50 | 2 | 20 | Steady-state (2) | ✓ | ✓ | ✗ | ✗ | ✓ | ✓ | ✓ | Siemens Energy SOFC |
| | | | | | | | | | | ✓ | ✓ | ✗ | ✗ | ✗ | ✓ | ✓ | 5 kW SOFC |
| | CSO (Xiong et al. 2020) | 2020 | 7 | MQD | 50,000 | N.M | ✗ | 50 | Electrochemical | ✓ | ✓ | ✗ | ✓ | ✓ | ✓ | ✗ | Siemens Energy SOFC |
| | | | | | | | | | | ✓ | ✗ | ✗ | ✓ | ✓ | ✓ | ✗ | 5 kW SOFC |

**Table 7** (continued)

| Family | Optimizer | Year | $N_{un}$ | AF | Tuned parameters' | | | $N_{IE}$ | Model | Simulated curves | | | Different conditions | | Statistical assessment | | Test cases |
|---|---|---|---|---|---|---|---|---|---|---|---|---|---|---|---|---|---|
| | | | | | IT | $N_p$ | others | | | V-I | P-I | I-t & V-t | $P_H$ | $T_{op}$ | Parametric | Non-parametric | |
| | ISO (El-Hay et al. 2019) | 2019 | 6 | MQD | 100 | N.M | 1 | 50 | Steady-state (2) | ✓ | ✓ | ✗ | ✗ | ✓ | ✓ | ✗ | Siemens Energy SOFC |
| | | | | | | | | | Steady-state (2) | ✓ | ✓ | ✗ | ✗ | ✗ | ✗ | ✗ | 100 kW SOFC |
| | | | | | | | | | Dynamic | ✗ | ✗ | ✓ | ✗ | ✗ | ✗ | ✗ | 100 kW SOFC |
| | GWO (Hao and Sobhani 2021) | 2021 | 7 | MQD | 50,000 | N.M | 3 | N.M | Electrochemical | ✓ | ✓ | ✗ | ✓ | ✓ | ✗ | ✗ | 5 kW SOFC |
| | EO (Rizk-Allah et al. 2021) | 2021 | 6 | MQD | 100 | 50 | 2 | 20 | Steady-state (2) | ✗ | ✗ | ✗ | ✗ | ✗ | ✓ | ✓ | Siemens Energy SOFC |
| | | | | | | | | | | ✗ | ✗ | ✗ | ✗ | ✗ | ✓ | ✓ | 5 kW SOFC |
| | GBO (Rizk-Allah et al. 2021) | 2021 | 6 | MQD | 100 | 50 | 3 | 20 | Steady-state (2) | ✗ | ✗ | ✗ | ✗ | ✗ | ✓ | ✓ | Siemens Energy SOFC |
| | | | | | | | | | | ✗ | ✗ | ✗ | ✗ | ✗ | ✓ | ✓ | 5 kW SOFC |
| | HBO (Yakout et al. 2022) | 2022 | 6 | MQD | 100 | 250 | 2 | 50 | Steady-state (2) | ✓ | ✓ | ✗ | ✗ | ✓ | ✓ | ✗ | Siemens Energy SOFC |
| | | | | | | | | | Steady-state (2) | ✓ | ✗ | ✗ | ✗ | ✗ | ✓ | ✗ | 100 kW SOFC |
| | | | | | | | | | Dynamic | ✗ | ✓ | ✓ | ✗ | ✗ | ✗ | ✗ | 100 kW SOFC |

**Table 7** (continued)

| Family | Optimizer | Year | $N_{un}$ | AF | Tuned parameters' | | | $N_{IE}$ | Model | Simulated curves | | | Different conditions | | Statistical assessment | | Test cases |
|---|---|---|---|---|---|---|---|---|---|---|---|---|---|---|---|---|---|
| | | | | | IT | $N_p$ | others | | | V-I | P-I | I-t & V-t | $P_H$ | $T_{op}$ | Parametric | Non-parametric | |
| Nature | BESO (Abaza et al. 2022) | 2022 | 7 | MQD | 250 | N.M | 2 | 30 | Electrochemical | ✓ | ✓ | ✗ | ✗ | ✓ | ✓ | ✗ | 5 kW SOFC |
| | CHA (Kele et al. 2022) | 2022 | 7 | MQD | 200 | 35 | 2 | 35 | Electrochemical | ✓ | ✓ | ✗ | ✓ | ✓ | ✓ | ✗ | 5 kW SOFC |
| | AVO (Bagal et al. 2021) | 2021 | 7 | MQD | N.M | N.M | 6 | N.M | Electrochemical | ✓ | ✓ | ✗ | ✓ | ✓ | ✓ | ✗ | 5 kW SOFC |
| | MPO (Yousri et al. 2021) | 2021 | 6 | MQD | 100 | 30 | ✗ | 30 | Steady-state (2) | ✓ | ✓ | ✗ | ✗ | ✓ | ✓ | ✓ | Siemens Energy SOFC |
| | | | | | | | | | Steady-state (2) | ✓ | ✓ | ✗ | ✗ | ✗ | ✗ | ✗ | 100 kW SOFC |
| | | | | | | | | | Dynamic | ✗ | ✗ | ✓ | ✗ | ✗ | ✗ | ✗ | 100 kW SOFC |
| | RFO (Luo and Shafiee 2021) | 2021 | 7 | MQD | 200 | 100 | 2 | 30 | Electrochemical | ✓ | ✓ | ✗ | ✓ | ✓ | ✗ | ✗ | 5 kW SOFC |
| | SSO (Wei & Stanford 2019) | 2019 | 6 | MQD | 100 | N.M | 3 | N.M | Steady-state (2) | ✓ | ✓ | ✗ | ✗ | ✓ | ✓ | ✓ | Siemens Energy SOFC |
| | | | | | | | | | Steady-state (2) | ✓ | ✓ | ✗ | ✗ | ✗ | ✓ | ✓ | 5 kW SOFC |
| | | | | | | | | | Dynamic | ✗ | ✗ | ✓ | ✗ | ✗ | ✗ | ✗ | 100 kW SOFC |
| | ALO (Ai et al. 2022) | 2022 | 7 | RMQD | 200 | 50 | ✗ | 12 | Electrochemical | ✓ | ✓ | ✗ | ✗ | ✗ | ✓ | ✓ | 5 kW SOFC |
| | EPO (Guo et al. 2022) | 2022 | 7 | OQD | 200 | 120 | 6 | 30 | Electrochemical | ✓ | ✓ | ✗ | ✓ | ✓ | ✗ | ✗ | 5 kW SOFC |
| | GTO (Yakout et al. 2022) | 2022 | 6 | MQD | 100 | 250 | 4 | 50 | Steady-state (2) | ✓ | ✓ | ✗ | ✗ | ✓ | ✓ | ✗ | Siemens Energy SOFC |
| | | | | | | | | | Steady-state (2) | ✓ | ✗ | ✗ | ✗ | ✗ | ✓ | ✗ | 100 kW SOFC |
| | | | | | | | | | Dynamic | ✗ | ✗ | ✓ | ✗ | ✗ | ✗ | ✗ | 100 kW SOFC |

*$N_{un}$, $N_p$, and $N_{IE}$ refer to the number of unknown parameters, population size, and algorithm independent executions, respectively

(a) Best AFs

(b) Average AFs

(c) Standard deviation values

(d) Computational performance ranking
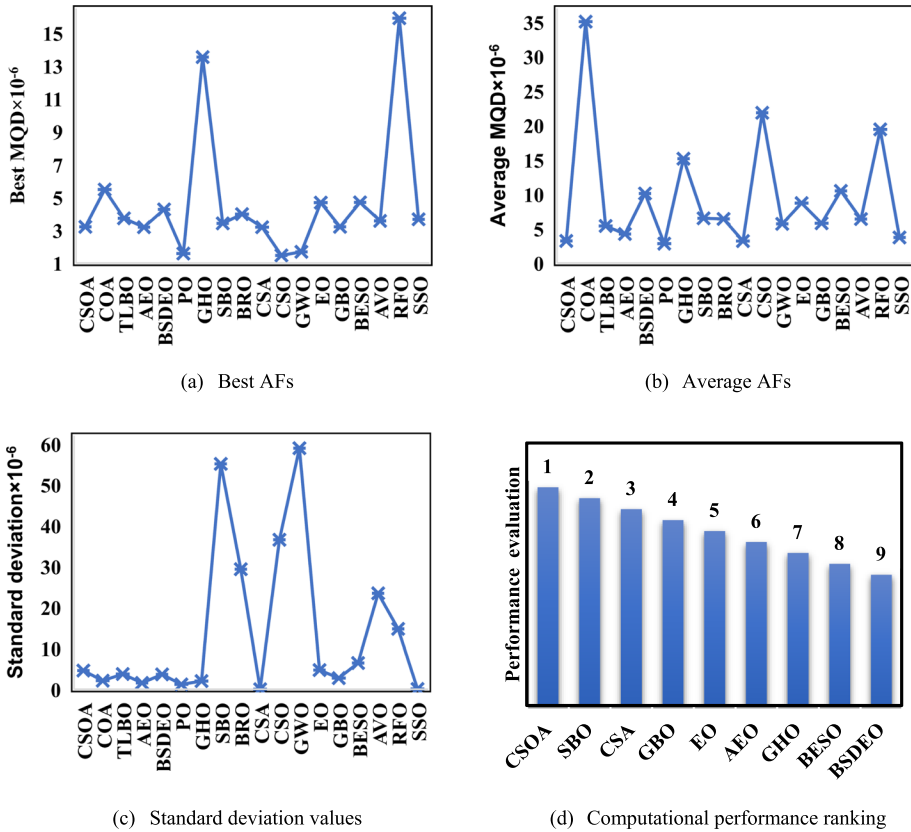
**Fig. 14** Statistical evaluation of MHOs for parameter estimation of 5 kW SOFCs stack

merits and limitations for specific tasks such that there is no unique algorithm that can deal with all engineering optimization problems. Additionally, there is still no solid answer, or it is quite difficult to decide that optimization method X is most suitable to optimization problem Y of certain characteristics such as degree of non-linearity, non-convex, multi-modality, separability of the control variables, high dimensionality etc. Till getting such an answer, attempts shall continue in these endeavors.

Among such effective trails, radial basis function neural network (Raj and Naik 2023b), Levenberg–Marquardt neural network (Rao et al. 2023), and adaptive neuro-fuzzy inference system (Raj and Naik 2023a) have proven advantageous characteristics, when engaged with heavy non-linear models. For instance, they don't require sophisticated high-order differential equations to accurately correlate output to input, they can efficiently simulate and predict the behavior of SOFCs through diverse operating circumstances. In addition, the authors in (Nama et al. 2023) proposed a new hybrid optimization methodology that integrates PSO with backtracking search optimizer (BSO) to mitigate the unbalance transition between exploration and exploitation. Furthermore, a recent version of slime mould optimizer supported by quadratic approximation is introduced in (Chakraborty et al. 2023) to dump stagnation into local solution. Another attempt, an enhanced moth-flame optimizer engaged with

(a)  V-I Curve
(b)  P-I Curve
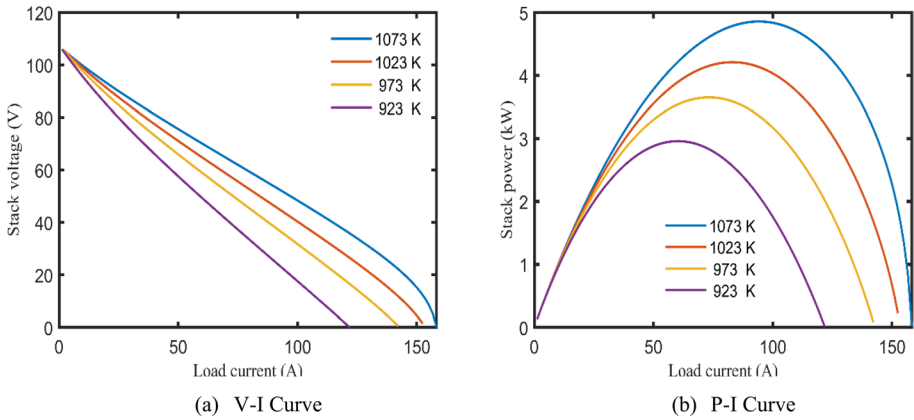
**Fig. 15** CSO-based steady-state response of SOFCs' stack at various temperatures



(a)  Load current variation
(b)  Stack voltage variation
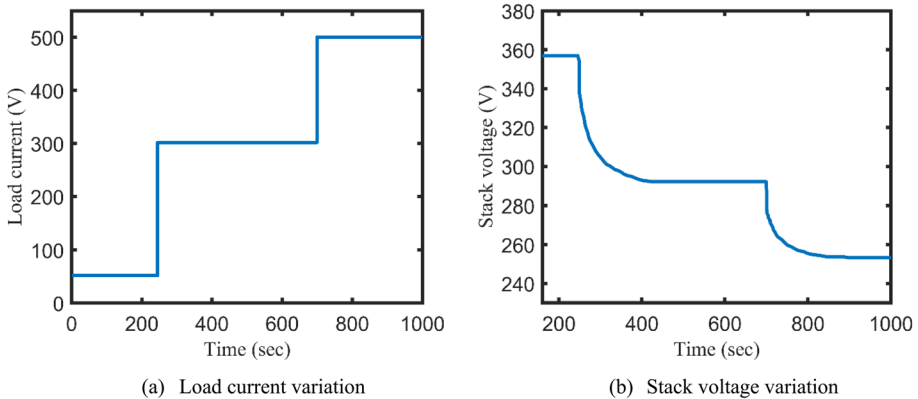
**Fig. 16** SBO-based dynamic response of SOFCs' stack

an upgraded dynamic opposite learning tactic is presented in (Sahoo et al. 2023) to avoid premature convergence. Additionally, new variants of BSO are proposed in (Nama and Saha 2022; Nama et al. 2022) to enhance its searching capability in the search space, especially for large dimensions problems. The reader is encouraged to browse (Chakraborty et al. 2022; Nama 2021, 2022; Saha et al. 2019; Sharma et al. 2022) for better comprehension of modern hybrid and improved optimization approaches applied in recent engineering problems.

### 5.2 Simulation Results

In addition, to provide the reader with a graphical explanation of how awesome the results of engaging MHOs in SOFC parameter estimation, Fig 15 and 16 reveal the polarization characteristics of SOFC based on certain MHOs (Pourrahmani and Gay 2021; Wang et al. 2022). In deep, the steady-state V-I and P-I curves of a tubular 5

kW SOFCs stack, based on CSO's outcomes, under various operating temperatures are introduced in Fig. 15a and b, respectively (Wu and Shafiee 2020; Xiong et al. 2020). Moreover, depending on SBO's methodology, Fig.16a and b offer the dynamic response of a 100 kW stack located in Netherlands, in terms of I and V vs simulation time curves, respectively (El-Hay et al. 2018; Santarelli et al. 2007). It's worth concluding that according to Fig. 15, the steady-state performance of SOFC is enhanced by increasing the temperature without exceeding its technical limits (Shi et al. 2020; Vigneysh and Kumarappan 2016). Besides, it's clear from Fig. 16 that the transient model can efficiently describe the impacts of load dynamics on SOFC.

## 6 Future Perspectives

Notwithstanding MHOs have exhibited promising outcomes in various engineering problems, the majority still suffer from getting trapped into local minima during the independent runs due to their high haphazardness. This results in low statistical performance, such as a high standard deviation. Even if some overcome such an issue, they may encounter slow convergence rates of the fitness function. Thus, developing novel metaheuristic-based optimization techniques, either single or hybrid, are imperative to keep up with the high nonlinearity and high dimensionality of SOFC's models. Moreover, attempts should be directed toward employing new machine learning and deep learning approaches to optimize SOFCs' performance, since they have a great ability to simulate the real physical attitude of SOFCs without any complicated mathematical formulations. Furthermore, such approaches can effectively anticipate SOFC response due to multiple disturbances and faults. On top of that, formulating new assessment functions can significantly contribute to an accurate evaluation of numerous employed optimizers. Finally, further experimental measurements at various operating conditions shall be recorded to magnify the precision of simulation and prediction.

## 7 Conclusion

This article undertakes a thorough review of the most recent metaheuristic optimizers engaged in SOFC parameter recognition, in terms of their performance, outcomes, and statistics. The contributions of this work can be represented in the following items:

- A detailed overview of several well-matured mathematical models that accurately describe the electrical behavior of SOFCs in either steady-state or dynamic operations.
- Deep illustration of 30 well-known recently dated MHOs that are employed for specifying the undefined parameters of SOFCs.
- Classification of these MHOs according to their based family, their motivation, their characteristics, and finally their outcomes in SOFC parameter identification.
- A summary of the different evaluation functions that have been adopted as a measure of algorithm robustness.
- Moreover, an inclusive comparison among these algorithms with a summary of their mathematical models besides enhanced amendments included in their methodology.
- Computational settings of each optimizer accompanied by the corresponding simulated test cases and their technical specs.

- Lastly, a validation check of such methodologies by utilizing two MHOs for enhancing both the steady-state and transient performances of actual test cases, namely the tubular 5 kW and 100 kW SOFCs stacks.

Consequently, this article can be considered as an outlet for the researcher to dedicate more attempts towards engaging novel artificial intelligence-based techniques for better emulating the electrical performance of SOFCs. Furthermore, innovating new assessment criteria is crucial to keep up with testing benchmarks that can properly and precisely evaluate such optimization techniques.

**Data Availability** Not applicable.

## Declarations

**Competing interests** The authors declare no competing interests.

**Research Involving Human and Animal Participants** The study did not involve humans or animals..

**Informed Consent** The study did not involve humans.

## References

Abaza A, El Sehiemy RA, Bayoumi ASA (2020) Optimal parameter estimation of solid oxide fuel cell model using coyote optimization algorithm. In: Recent advances in engineering mathematics and physics: proceedings of the international conference RAEMP 2019

Abaza A, El Sehiemy RA, El-Fergany A, Bayoumi ASA (2022) Optimal parameter estimation of solid oxide fuel cells model using bald eagle search optimizer. Int J Energy Res 46(10):13657–13669

Abdel-Basset M, Mohamed R, Abouhawwah M (2022) Hybrid marine predators algorithm for image segmentation: analysis and validations. Artif Intell Rev 1–53

Abou El-Ela AA, El-Sehiemy RA, Shaheen AM, Diab AE-G (2021) Enhanced coyote optimizer-based cascaded load frequency controllers in multi-area power systems with renewable. Neural Comput Appl 33:8459–8477

Ai X, Yue Y, Xu H (2022) Grasshopper optimization algorithms for parameter extraction of solid oxide fuel cells. Front Energy Res 10:853991

Akan T, Agahian S, Dehkharghani R (2022) Battle royale optimizer for solving binary optimization problems. Softw Impacts 12:100274

Al-Betar MA, Awadallah MA, Makhadmeh SN, Alyasseri ZAA, Al-Naymat G, Mirjalili S (2023) Marine predators algorithm: a review. **Arch Comput Methods Eng** 1–31

Alsaidan I, Shaheen MA, Hasanien HM, Alaraj M, Alnafisah AS (2022) A PEMFC model optimization using the enhanced bald eagle algorithm. Ain Shams Eng J 13(6):101749

Amezquita L, Castillo O, Soria J, Cortes-Antonio P (2023) New variants of the multi-verse optimizer algorithm adapting chaos theory in benchmark optimization. Symmetry 15(7):1319

Arenas-Acuña CA, Rodriguez-Contreras JA, Montoya OD, Rivas-Trujillo E (2021) Black-hole optimization applied to the parametric estimation in distribution transformers considering voltage and current measures. Computers 10(10):124

Ashraf H, Abdellatif SO, Elkholy MM, El-Fergany AA (2022a) Computational techniques based on artificial intelligence for extracting optimal parameters of PEMFCs: survey and insights. Arch Comput Methods Eng 29(6):3943–3972

Ashraf H, Abdellatif SO, Elkholy MM, El-Fergany AA (2022b) Honey badger optimizer for extracting the ungiven parameters of PEMFC model: steady-state assessment. Energy Convers Manage 258:115521

Ashraf H, Elkholy MM, Abdellatif SO, El-Fergany AA (2022c) Synergy of neuro-fuzzy controller and tuna swarm algorithm for maximizing the overall efficiency of PEM fuel cells stack including dynamic performance. Energy Convers Manageme X 16:100301

Ashraf MM, Malik TN (2020) A hybrid teaching–learning-based optimizer with novel radix-5 mapping procedure for minimum cost power generation planning considering renewable energy sources and reducing emission. Electr Eng 102(4):2567–2582

Askarzadeh A (2017) Solving electrical power system problems by harmony search: a review. Artif Intell Rev 47(2):217–251

Ayodele T, Ogunjuyigbe A, Ekoh E (2016) Evaluation of numerical algorithms used in extracting the parameters of a single-diode photovoltaic model. Sustainable Energy Technol Assess 13:51–59

Azizi M, Mousavi Ghasemi SA, Ejlali RG, Talatahari S (2020) Optimum design of fuzzy controller using hybrid ant lion optimizer and Jaya algorithm. Artif Intell Rev 53:1553–1584

Azizipanah-Abarghooee R, Niknam T, Bavafa F, Zare M (2014) Short-term scheduling of thermal power systems using hybrid gradient based modified teaching–learning optimizer with black hole algorithm. Electric Power Syst Res 108:16–34

Babu TS, Ram JP, Sangeetha K, Laudani A, Rajasekar N (2016) Parameter extraction of two diode solar PV model using Fireworks algorithm. Sol Energy 140:265–276

Badr AA, Saafan MM, Abdelsalam MM, Haikal AY (2023) Novel variants of grasshopper optimization algorithm to solve numerical problems and demand side management in smart grids. Artif Intell Rev 1–54

Bagal HA, Soltanabad YN, Dadjuo M, Wakil K, Zare M, Mohammed AS (2021) SOFC model parameter identification by means of modified african vulture optimization algorithm. Energy Rep 7:7251–7260

Bavarian M, Soroush M, Kevrekidis IG, Benziger JB (2010) Mathematical modeling, steady-state and dynamic behavior, and control of fuel cells: a review. Ind Eng Chem Res 49(17):7922–7950

Bayzidi H, Talatahari S, Saraee M, Lamarche C-P (2021) Social network search for solving engineering optimization problems. Comput Intell Neurosci 2021:1–32

Bessekon Y, Zielke P, Wulff AC, Hagen A (2019) Simulation of a SOFC/Battery powered vehicle. Int J Hydrogen Energy 44(3):1905–1918

Caliandro P, Nakajo A, Diethelm S (2019) Model-assisted identification of solid oxide cell elementary processes by electrochemical impedance spectroscopy measurements. J Power Sources 436:226838

Cao H, Deng Z, Li X, Yang J, Qin Y (2010) Dynamic modeling of electrical characteristics of solid oxide fuel cells using fractional derivatives. Int J Hydrogen Energy 35(4):1749–1758

Chakraborty P, Nama S, Saha AK (2023) A hybrid slime mould algorithm for global optimization. Multimed Tools Appl 82(15):22441–22467

Chakraborty S, Nama S, Saha AK (2022) An improved symbiotic organisms search algorithm for higher dimensional optimization problems. Knowl-Based Syst 236:107779

Chakraborty UK (2009) Static and dynamic modeling of solid oxide fuel cell using genetic programming. Energy 34(6):740–751

Chan S, Low C, Ding O (2002) Energy and exergy analysis of simple solid-oxide fuel-cell power systems. J Power Sources 103(2):188–200

Chang L, Li M, Qian L, de Oliveira GG (2023) Developed multi-objective honey badger optimizer: Application to optimize proton exchange membrane fuel cells-based combined cooling, heating, and power system. Int J Hydrog Energy

Chen K, Laghrouche S, Djerdir A (2019) Degradation model of proton exchange membrane fuel cell based on a novel hybrid method. Appl Energy 252:113439

Chen X, Yu K, Du W, Zhao W, Liu G (2016) Parameters identification of solar cell models using generalized oppositional teaching learning based optimization. Energy 99:170–180

Cheng R, Jin Y (2014) A competitive swarm optimizer for large scale optimization. IEEE Trans Cybern 45(2):191–204

Chintam JR, Daniel M (2018) Real-power rescheduling of generators for congestion management using a novel satin bowerbird optimization algorithm. Energies 11(1):183

Cigolotti V, Genovese M, Fragiacomo P (2021) Comprehensive review on fuel cell technology for stationary applications as sustainable and efficient poly-generation energy systems. Energies 14(16):4963

Civicioglu P, Besdok E (2019) Bernstain-search differential evolution algorithm for numerical function optimization. Expert Syst Appl 138:112831

Dai C, Chen W, Cheng Z, Li Q, Jiang Z, Jia J (2011) Seeker optimization algorithm for global optimization: a case study on optimal modelling of proton exchange membrane fuel cell (PEMFC). Int J Electr Power Energy Syst 33(3):369–376

Daoud MS, Shehab M, Al-Mimi HM, Abualigah L, Zitar RA, Shambour MKY (2023) Gradient-based optimizer (GBO): a review, theory, variants, and applications. Arch Comput Methods Eng 30(4):2431–2449

de Melo SVS, Yahyaoui I, Fardin JF, Encarnação LF, Tadeo F (2018) Power unit SOFC-MTG model in electromagnetic transient software PSCAD. Int J Hydrogen Energy 43(10):5386–5397

Draz A, Elkholy MM, El-Fergany AA (2021) Soft computing methods for attaining the protective device coordination including renewable energies: review and prospective. Arch Comput Methods Eng 1–22

Draz A, Elkholy MM, El-Fergany AA (2023a) Automated settings of overcurrent relays considering transformer phase shift and distributed generators using gorilla troops optimizer. Mathematics 11(3):774

Draz A, Othman AM, El-Fergany AA (2023b) State-of-the-art with numerical analysis on electric fast charging stations: infrastructures, standards, techniques, and challenges. Renew. Energy Focus 100499

Duan B, Cao Q, Afshar N (2019) Optimal parameter identification for the proton exchange membrane fuel cell using Satin Bowerbird optimizer. Int J Energy Res 43(14):8623–8632

El-Fergany A (2015) Study impact of various load models on DG placement and sizing using backtracking search algorithm. Appl Soft Comput 30:803–811

El-Fergany AA (2021) Parameters identification of PV model using improved slime mould optimizer and Lambert W-function. Energy Rep 7:875–887

El-Fergany AA, Hasanien HM (2015) Single and multi-objective optimal power flow using grey wolf optimizer and differential evolution algorithms. Electri Power Compon Syst 43(13):1548–1559

El-Hay E, El-Hameed M, El-Fergany A (2018) Steady-state and dynamic models of solid oxide fuel cells based on Satin Bowerbird optimizer. Int J Hydrogen Energy 43(31):14751–14761

El-Hay E, El-Hameed M, El-Fergany A (2019) Optimized parameters of SOFC for steady state and transient simulations using interior search algorithm. Energy 166:451–461

El-Dabah MA, El-Sehiemy RA, Becherif M, Ebrahim M (2021) Parameter estimation of triple diode photovoltaic model using an artificial ecosystem-based optimizer. Int Trans Electr Energy Syst 31(11):e13043

El-Hameed MA, El-Fergany AA (2016) Water cycle algorithm-based load frequency controller for interconnected power systems comprising non-linearity. IET Gener Transm Distrib 10(15):3950–3961

Elkholy MM, El-Hameed M, El-Fergany A (2018) Harmonic analysis of hybrid renewable microgrids comprising optimal design of passive filters and uncertainties. Electric Power Syst Res 163:491–501

Elsisi M (2022) Improved grey wolf optimizer based on opposition and quasi learning approaches for optimization: case study autonomous vehicle including vision system. Artif Intell Rev 55(7):5597–5620

Emad D, El-Hameed M, El-Fergany A (2021) Optimal techno-economic design of hybrid PV/wind system comprising battery energy storage: case study for a remote area. Energy Convers Manage 249:114847

Fahmy HM, Sweif RA, Hasanien HM, Tostado-Véliz M, Alharbi M, Jurado F (2023) Parameter Identification of Lithium-Ion battery model based on African vultures optimization algorithm. Mathematics 11(9):2215

Fathy A (2023) Bald eagle search optimizer-based energy management strategy for microgrid with renewable sources and electric vehicles. Appl Energy 334:120688

Fathy A, Rezk H (2020) Robust electrical parameter extraction methodology based on interior search optimization algorithm applied to supercapacitor. ISA Trans 105:86–97

Fathy A, Rezk H (2022) Political optimizer based approach for estimating SOFC optimal parameters for static and dynamic models. Energy 238:122031

Fathy A, Rezk H, Ferahtia S, Ghoniem RM, Alkanhel R (2023) An efficient honey badger algorithm for scheduling the microgrid energy management. Energy Rep 9:2058–2074

Fathy A, Rezk H, Ramadan HSM (2020) Recent moth-flame optimizer for enhanced solid oxide fuel cell output power via optimal parameters extraction process. Energy 207:118326

Feng Z-K, Niu W-J, Liu S (2021) Cooperation search algorithm: a novel metaheuristic evolutionary intelligence algorithm for numerical optimization and engineering optimization problems. Appl Soft Comput 98:106734

Gebregergis A, Pillay P, Bhattacharyya D, Rengaswemy R (2008) Solid oxide fuel cell modeling. IEEE Trans Industr Electron 56(1):139–148

Ghaedi A, Bardsiri AK, Shahbazzadeh MJ (2023) Cat hunting optimization algorithm: a novel optimization algorithm. Evol Intel 16(2):417–438

Ghanem RS, Nousch L, Richter M (2022) Modeling of a grid-independent set-up of a PV/SOFC micro-CHP system combined with a seasonal energy storage for residential applications. Energies 15(4):1388

Ghavidel HF, Mousavi-G SM (2022) Modeling analysis, control, and type-2 fuzzy energy management strategy of hybrid fuel cell-battery-supercapacitor systems. J Energy Storage 51:104456

Gnetchejo PJ, Ndjakomo Essiane S, Dadjé A, Mbadjoun Wapet DE, Ele P, Chen Z (2023) Improved social network search algorithm coupled with Lagrange method for extracting the best parameter of photovoltaic modules and array. Int J Energy Environ Eng 14(3):525–535

Gomes RCM, Vitorino MA, de Rossiter Corrêa MB, Fernandes DA, Wang R (2016) Shuffled complex evolution on photovoltaic parameter extraction: A comparative analysis. IEEE Trans Sustain Energy 8(2):805–815

Gong W, Cai Z, Yang J, Li X, Jian L (2014) Parameter identification of an SOFC model with an efficient, adaptive differential evolution algorithm. Int J Hydrogen Energy 39(10):5083–5096

Gouda EA, Kotb MF, El-Fergany AA (2021) Jellyfish search algorithm for extracting unknown parameters of PEM fuel cell models: steady-state performance and analysis. Energy 221:119836

Guo H, Gu W, Khayatnezhad M, Ghadimi N (2022) Parameter extraction of the SOFC mathematical model based on fractional order version of dragonfly algorithm. Int J Hydrogen Energy 47(57):24059–24068

Hamada AT, Orhan MF, Kannan AM (2023) Alkaline fuel cells: status and prospects. Energy Rep 9:6396–6418

Han W, Li D, Yu D, Ebrahimian H (2023) Optimal parameters of PEM fuel cells using chaotic binary shark smell optimizer. Energy Sources, Part A: Recovery, Utili, Environ Eff 45(3):7770–7784

Hao P, Sobhani B (2021) Application of the improved chaotic grey wolf optimization algorithm as a novel and efficient method for parameter estimation of solid oxide fuel cells model. Int J Hydrogen Energy 46(73):36454–36465

Hasanien HM, Alsaleh I, Tostado-Véliz M, Alassaf A, Alateeq A, Jurado F (2023) Optimal parameters estimation of lithium-ion battery in smart grid applications based on gazelle optimization algorithm. Energy 285:129509

Hatta AM, Zain AM, Sallehuddin R, Shayfull Z, Yusoff Y (2019) Recent studies on optimisation method of Grey Wolf Optimiser (GWO): a review (2014–2017). Artif Intell Rev 52:2651–2683

Inci M, Türksoy Ö (2019) Review of fuel cells to grid interface: configurations, technical challenges and trends. J Clea Prod 213:1353–1370

Ismael I, El-Fergany AA, Gouda EA, Kotb MF (2023) Cooperation search algorithm for optimal parameters identification of SOFCs feeding electric vehicle at steady and dynamic modes. Int J Hydrogen Energy

Jawad NH, Yahya AA, Al-Shathr AR, Salih HG, Rashid KT, Al-Saadi S, AbdulRazak AA, Salih IK, Zrelli A, Alsalhy QF (2022) Fuel cell types, properties of membrane, and operating conditions: a review. Sustainability 14(21):14653

Jia H, Taheri B (2021) Model identification of solid oxide fuel cell using hybrid Elman neural network/quantum pathfinder algorithm. Energy Rep 7:3328–3337

Jiang S, Wang C, Zhang C, Bai H, Xu L (2019) Adaptive estimation of road slope and vehicle mass of fuel cell vehicle. Etransportation 2:100023

Jolaoso LA, Bello IT, Ojelade OA, Yousuf A, Duan C, Kazempoor P (2023). Operational and scaling-up barriers of SOEC and mitigation strategies to boost H2 production-a comprehensive review. Int J Hydrogen Energy

Kahia H, Saadi A, Herbadji A, Herbadji D, Ramadhan HM (2023) Accurate estimation of PEMFC state of health using modified hybrid artificial neural network models. J New Mater Electrochem Syst 26(1):32–41

Kalavani F, Zamani-Gargari M, Mohammadi-Ivatloo B, Rasouli M (2019) A contemporary review of the applications of nature-inspired algorithms for optimal design of automatic generation control for multi-area power systems. Artif Intell Rev 51:187–218

Karamnejadi Azar K, Kakouee A, Mollajafari M, Majdi A, Ghadimi N, Ghadamyari M (2022) Developed design of battle royale optimizer for the optimum identification of solid oxide fuel cell. Sustainability 14(16):9882

Karanfil G (2020) Importance and applications of DOE/optimization methods in PEM fuel cells: a review. Int J Energy Res 44(1):4–25

Kasaeian A, Javidmehr M, Mirzaie MR, Fereidooni L (2023) Integration of solid oxide fuel cells with solar energy systems: a review. Appl Ther Eng 120117

Kele C, Xinmei W, Youssefi N (2022) Model parameter estimation of SOFCs using a modified cat optimization algorithm. Sustainable Energy Technol Assess 52:102176

Khalid OW, Isa NAM, Sakim HAM (2023) Emperor penguin optimizer: a comprehensive review based on state-of-the-art meta-heuristic algorithms. Alex Eng J 63:487–526

Korkmaz SA, Çetinkaya SA, Yuksel O, Konur O, Erginer KE, Colpan CO (2023) Comparison of various metaheuristic algorithms to extract the optimal PEMFC modeling parameters. Int J Hydrogen Energy

Lakhina U, Elamvazuthi I, Badruddin N, Jangra A, Truong B-H, Guerrero JM (2023) A cost-effective multi-verse optimization algorithm for efficient power generation in a microgrid. Sustainability 15(8):6358

Lamagna M, Groppi D, Nastasi B (2023) Reversible solid oxide cells applications to the building sector. Int J Hydrogen Energy

Lee D, Quach T-Q, Israel TP, Ahn KY, Bae Y, Kim YS (2022) Analysis of start-up behavior based on the dynamic simulation of an SOFC–engine hybrid system. Energy Convers Manage 272:116384

Lee J, Lin K-YA, Jung S, Kwon EE (2023a) Hybrid renewable energy systems involving thermochemical conversion process for waste-to-energy strategy. Chem Eng J 452:139218

Lee JI, Yoon BY, Cha SW (2023b) Analysis of solid oxide fuel cell hybrid power system in marine application for $CO_2$ reduction. Energy Rep 9:3072–3081

Liu L, Qian J, Hua L, Zhang B (2022) System estimation of the SOFCs using fractional-order social network search algorithm. Energy 255:124516

Lokhande AA, Rathore V, Patel R, Dudhate R, Kulkarni K (2023) Hydrogen fuel cell: parametric analysis of their stockpiling and different types. Mater Today: Proc 72:1236–1239

Luo R, Shafiee M (2021) The application of metaheuristics in optimal parameter identification of solid oxide fuel cell. Energy Rep 7:2563–2573

Ma R, Yang T, Breaz E, Li Z, Briois P, Gao F (2018) Data-driven proton exchange membrane fuel cell degradation predication through deep learning method. Appl Energy 231:102–115

Mahmoud I, Hasanien HM, Turky RA, Omran WA (2023) Energy management system for islanded multi-microgrids using a two-stage optimization scheme based on political optimizer. IET Renew Power Gener 17(7):1713–1730

Mehran MT, Khan MZ, Song R-H, Lim T-H, Naqvi M, Raza R, Zhu B, Hanif MB (2023) A comprehensive review on durability improvement of solid oxide fuel cells for commercial stationary power generation systems. Appl Energy 352:121864

Mirjalili SZ, Mirjalili S, Saremi S, Faris H, Aljarah I (2018) Grasshopper optimization algorithm for multi-objective optimization problems. Appl Intell 48:805–820

Mitra U, Arya A, Gupta S (2023) A comprehensive and comparative review on parameter estimation methods for modelling proton exchange membrane fuel cell. Fuel 335:127080

Mohammed RH, Ismaiel AM, Elnaghi BE, Dessouki ME (2023) African vulture optimizer algorithm based vector control induction motor drive system. Int J Electr Comput Eng (2088–8708), 13(3)

Nama S (2021) A modification of I-SOS: performance analysis to large scale functions. Appl Intell 51(11):7881–7902

Nama S (2022) A novel improved SMA with quasi reflection operator: Performance analysis, application to the image segmentation problem of Covid-19 chest X-ray images. Appl Soft Comput 118:108483

Nama S, Saha AK (2020) A new parameter setting-based modified differential evolution for function optimization. Int J Model, Simul, Sci Comput 11(04):2050029

Nama S, Saha AK (2022) A bio-inspired multi-population-based adaptive backtracking search algorithm. Cogn Comput 14(2):900–925

Nama S, Saha AK, Chakraborty S, Gandomi AH, Abualigah L (2023) Boosting particle swarm optimization by backtracking search algorithm for optimization problems. Swarm Evol Comput 79:101304

Nama S, Saha AK, Sharma S (2020) A hybrid TLBO algorithm by quadratic approximation for function optimization and its application. In: Recent trends and advances in artificial intelligence and internet of things, pp 291–341

Nama S, Sharma S, Saha AK, Gandomi AH (2022) A quantum mutation-based backtracking search algorithm. Artif Intell Rev 1–55

Noren D, Hoffman MA (2005) Clarifying the Butler-Volmer equation and related approximations for calculating activation losses in solid oxide fuel cell models. J Power Sources 152:175–181

Ohenoja M, Leiviskä K (2020) Observations on the parameter estimation problem of polymer electrolyte membrane fuel cell polarization curves. Fuel Cells 20(5):516–526

Oryshchyn D, Harun NF, Tucker D, Bryden KM, Shadle L (2018) Fuel utilization effects on system efficiency in solid oxide fuel cell gas turbine hybrid systems. Appl Energy 228:1953–1965

Pan J-S, Hu P, Snášel V, Chu S-C (2023) A survey on binary metaheuristic algorithms and their engineering applications. Artif Intell Rev 56(7):6101–6167

Pandya SB, Jariwala HR (2022) Hybrid renewable energy resources incorporated optimal power flow using single phase multi-group teaching learning-based optimiser. Int J Comput Aided Eng Technol 17(4):361–387

Perna A, Minutillo M, Jannelli E, Cigolotti V, Nam S, Han J (2018) Design and performance assessment of a combined heat, hydrogen and power (CHHP) system based on ammonia-fueled SOFC. Appl Energy 231:1216–1229

Połap D, Woźniak M (2021) Red fox optimization algorithm. Expert Syst Appl 166:114107

Pourrahmani H, Gay M (2021) Electric vehicle charging station using fuel cell technology: two different scenarios and thermodynamic analysis. Energy Rep 7:6955–6972

Priya K, Sathishkumar K, Rajasekar N (2018) A comprehensive review on parameter estimation techniques for proton exchange membrane fuel cell modelling. Renew Sustain Energy Rev 93:121–144

Prokop TA, Berent K, Iwai H, Szmyd JS, Brus G (2018) A three-dimensional heterogeneity analysis of electrochemical energy conversion in SOFC anodes using electron nanotomography and mathematical modeling. Int J Hydrogen Energy 43(21):10016–10030

Rahmati K, Taherinasab S (2023) The importance of reconfiguration of the distribution network to achieve minimization of energy losses using the dragonfly algorithm. e-Prime-Adv Electr Eng, Electron Energy, 100270

Raj RDA, Naik KA (2023a) Priority queue-based switching matrix algorithm for adaptive neuro-fuzzy inference system assisted MPPT controlled PV system. Energy Convers Manage 293:117519

Raj RDA, Naik KA (2023b) Solar array optimization using cryptographic Fibonacci transformation for global power enhancement and ease of MPPT controllers. Energ Technol 11(9):2300380

Rao CV, Raj RDA, Anil Naik K (2023) A novel hybrid image processing-based reconfiguration with RBF neural network MPPT approach for improving global maximum power and effective tracking of PV system. Int J Circuit Theory Appl

Rao Y, Shao Z, Ahangarnejad AH, Gholamalizadeh E, Sobhani B (2019) Shark smell optimizer applied to identify the optimal parameters of the proton exchange membrane fuel cell model. Energy Convers Manage 182:1–8

Ren H, Hou X, Jia Z, Mashhadi A (2023) A new optimal energy management strategy of microgrids using chaotic map-based chameleon swarm algorithm. IET Renew Power Gener

Ren X (2022) Assessment and conceptual design of a SOFC/TIG/TEG-based hybrid propulsion system for a small UAV. Int J Energy Res 46(10):13336–13355

Rezk H, Olabi AG, Ghoniem RM, Abdelkareem MA (2023) Optimized fractional maximum power point tracking using bald eagle search for thermoelectric generation system. Energies 16(10):4064

Rizk-Allah RM, Abdelwanis MI, El-Sehiemy RA, Abd-Elrazek AS (2023) An interior search algorithm based on chaotic and crossover strategies for parameter extraction of polyphase induction machines. Neural Comput Appl 35(9):6647–6664

Rizk-Allah RM, El-Hameed MA, El-Fergany AA (2021) Model parameters extraction of solid oxide fuel cells based on semi-empirical and memory-based chameleon swarm algorithm. Int J Energy Res 45(15):21435–21450

Rossi I, Traverso A, Tucker D (2019) SOFC/Gas turbine hybrid system: a simplified framework for dynamic simulation. Appl Energy 238:1543–1550

Rupiper LN, Skabelund BB, Ghotkar R, Milcarek RJ (2022) Impact of fuel type on the performance of a solid oxide fuel cell integrated with a gas turbine. Sustainable Energy Technol Assess 51:101959

Safari A, Shahsavari H, Babaei F (2018) Optimal design of controllers for power network connected SOFC using of multi-objective PSO. Serbian J Electr Eng 15(2):145–163

Saha A, Nama S, Ghosh S (2019) Application of HSOS algorithm on pseudo-dynamic bearing capacity of shallow strip footing along with numerical analysis. Int J Geotech Eng

Sahoo SK, Saha AK, Nama S, Masdari M (2023) An improved moth flame optimization algorithm based on modified dynamic opposite learning strategy. Artif Intell Rev 56(4):2811–2869

Samir M, Singh G, Ahamad N (2022) Tilt integral derivative controller optimized by battle royale optimization for wind generator connected to grid. Indonesian J Electr Eng Inform (IJEEI) 10(2):302–316

Santarelli M, Leone P, Calì M, Orsello G (2007) Experimental evaluation of the sensitivity to fuel utilization and air management on a 100 kW SOFC system. J Power Sources 171(1):155–168

Sarmah P, Gogoi T, Das R (2017) Estimation of operating parameters of a SOFC integrated combined power cycle using differential evolution based inverse method. Appl Therm Eng 119:98–107

Sazali N, Wan Salleh WN, Jamaludin AS, Mhd Razali MN (2020) New perspectives on fuel cell technology: a brief review. Membranes 10(5):99

Shaheen A, El-Sehiemy R, El-Fergany A, Ginidi A (2023a) Fuel-cell parameter estimation based on improved gorilla troops technique. Sci Rep 13(1):8685

Shaheen A, Elsayed A, Ginidi A, El-Sehiemy R, Elattar E (2022) Reconfiguration of electrical distribution network-based DG and capacitors allocations using artificial ecosystem optimizer: practical case study. Alex Eng J 61(8):6105–6118

Shaheen AM, Ginidi AR, El-Sehiemy RA, El-Fergany A, Elsayed AM (2023) Optimal parameters extraction of photovoltaic triple diode model using an enhanced artificial gorilla troops optimizer. Energy 129034

Sharma S, Chakraborty S, Saha A, Nama S, Sahoo S (2022) mLBOA: a modified butterfly optimization algorithm with lagrange interpolation for global optimization. J Bionic Eng

Shi H, Li J, Zafetti N (2020) New optimized technique for unknown parameters selection of SOFC using converged grass fibrous root optimization algorithm. Energy Rep 6:1428–1437

Singla M, Gupta J, Nijhawan P (2019) Comparative study on backpropagation and levenberg marquardt algorithm on short term load forecasting. Int J Adv Trends Comput Sci Eng 8(2):194–202

Sohani A, Naderi S, Torabi F (2019) Comprehensive comparative evaluation of different possible optimization scenarios for a polymer electrolyte membrane fuel cell. Energy Convers Manage 191:247–260

Suresh V, Jasinski M, Leonowicz Z, Kaczorowska D, Reddy KH (2021) Political-optimizer-based energy-management system for microgrids. Electronics 10(24):3119

Talaat M, Elkholy M, Alblawi A, Said T (2023) Artificial intelligence applications for microgrids integration and management of hybrid renewable energy sources. Artif Intell Rev 1–55

Vigneysh T, Kumarappan N (2016) Autonomous operation and control of photovoltaic/solid oxide fuel cell/battery energy storage based microgrid using fuzzy logic controller. Int J Hydrogen Energy 41(3):1877–1891

Wang Y, Li S, Sun H, Huang C, Youssefi N (2022) The utilization of adaptive African vulture optimizer for optimal parameter identification of SOFC. Energy Rep 8:551–560

Wang Y, Yu Y, Cao S, Zhang X, Gao S (2020) A review of applications of artificial intelligent algorithms in wind farms. Artif Intell Rev 53:3447–3500

Wei Y, Stanford RJ (2019) Parameter identification of solid oxide fuel cell by chaotic binary shark smell optimization method. Energy 188:115770

Wu Q, Shafiee M (2020) Modeling and optimization of SOFC based on metaheuristics. Int J Electrochem Sci 15:11008–11023

Wu Z, Tan P, Chen B, Cai W, Chen M, Xu X, Zhang Z, Ni M (2019) Dynamic modeling and operation strategy of an NG-fueled SOFC-WGS-TSA-PEMFC hybrid energy conversion system for fuel cell vehicle by using MATLAB/SIMULINK. Energy 175:567–579

Xiong G, Shi D (2018) Orthogonal learning competitive swarm optimizer for economic dispatch problems. Appl Soft Comput 66:134–148

Xiong G, Zhang J, Shi D, He Y (2018) Parameter identification of solid oxide fuel cells with ranking teaching-learning based algorithm. Energy Convers Manage 174:126–137

Xiong G, Zhang J, Shi D, Yuan X (2020) A simplified competitive swarm optimizer for parameter identification of solid oxide fuel cells. Energy Convers Manage 203:112204

Xiong G, Zhang J, Shi D, Zhu L, Yuan X (2021) Optimal identification of solid oxide fuel cell parameters using a competitive hybrid differential evolution and Jaya algorithm. Int J Hydrogen Energy 46(9):6720–6733

Xu D, Jiang B, Liu F (2016) Improved data driven model free adaptive constrained control for a solid oxide fuel cell. IET Control Theory Appl 10(12):1412–1419

Yakout AH, Kotb H, AboRas KM, Hasanien HM (2022) Comparison among different recent metaheuristic algorithms for parameters estimation of solid oxide fuel cell: steady-state and dynamic models. Alex Eng J 61(11):8507–8523

Yang B, Chen Y, Guo Z, Wang J, Zeng C, Li D, Shu H, Shan J, Fu T, Zhang X (2021a) Levenberg-Marquardt backpropagation algorithm for parameter identification of solid oxide fuel cells. Int J Energy Res 45(12):17903–17923

Yang B, Guo Z, Yang Y, Chen Y, Zhang R, Su K, Shu H, Yu T, Zhang X (2021b) Extreme learning machine based meta-heuristic algorithms for parameter extraction of solid oxide fuel cells. Appl Energy 303:117630

Yang B, Wang J, Yu L, Shu H, Yu T, Zhang X, Yao W, Sun L (2020) A critical survey on proton exchange membrane fuel cell parameter estimation using meta-heuristic algorithms. J clean Prod 265:121660

Yang B, Wang J, Zhang M, Shu H, Yu T, Zhang X, Yao W, Sun L (2020b) A state-of-the-art survey of solid oxide fuel cell parameter identification: modelling, methodology, and perspectives. Energy Convers Manage 213:112856

Yang B, Zeng C, Wang L, Guo Y, Chen G, Guo Z, Chen Y, Li D, Cao P, Shu H (2021c) Parameter identification of proton exchange membrane fuel cell via Levenberg-Marquardt backpropagation algorithm. Int J Hydrogen Energy 46(44):22998–23012

Yatoo MA, Habib F, Malik AH, Qazi MJ, Ahmad S, Ganayee MA, Ahmad Z (2023) Solid-oxide fuel cells: a critical review of materials for cell components. MRS Comm 1–7

Yousri D, Hasanien HM, Fathy A (2021) Parameters identification of solid oxide fuel cell for static and dynamic simulation using comprehensive learning dynamic multi-swarm marine predators algorithm. Energy Convers Manage 228:113692

Zeghdi Z, Barazane L, Bekakra Y, Larabi A (2022) Improved backstepping control of a DFIG based wind energy conversion system using ant lion optimizer algorithm. Period Polytech Electr Eng Comput Sci 66(1):43–59

Zhang Q, Bu X, Zhan Z-H, Li J, Zhang H (2023) An efficient optimization state-based coyote optimization algorithm and its applications. Appl Soft Comput 110827

Zhang X, Lin Q (2022) Information-utilization strengthened equilibrium optimizer. Artifi Intell Rev 1–34

Zhao J, Zhang D, He Q, Li L (2023) A hybrid-strategy-improved dragonfly algorithm for the parameter identification of an SDM. Sustainability 15(15):11791

Zhou H, Wu X, Li Y, Fan Z, Chen W, Mao J, Deng P, Wik T (2024) Model optimization of a high-power commercial PEMFC system via an improved grey wolf optimization method. Fuel 357:129589

Zhou J, Xu Z (2023) Optimal sizing design and integrated cost-benefit assessment of stand-alone microgrid system with different energy storage employing chameleon swarm algorithm: a rural case in Northeast China. Renew Energy 202:1110–1137

Zhu J, Wu X, Sun K, Han M (2021) An Optimized Strategy for Fuel Cell Degradation Control in SOFC Power Systems. ECS Trans 103(1):1033

Zhu L, Zhang L, Virkar AV (2015) A parametric model for solid oxide fuel cells based on measurements made on cell materials and components. J Power Sources 291:138–155